Star Formation Histories of the Large and Small Magellanic Clouds

A DISSERTATION
SUBMITTED TO THE FACULTY OF THE GRADUATE SCHOOL
OF THE UNIVERSITY OF MINNESOTA
BY

Kyle Brian Neary

IN PARTIAL FULFILLMENT OF THE REQUIREMENTS
FOR THE DEGREE OF
Doctor of Philosophy

Dr. Evan D. Skillman, Advisor

May, 2014

Acknowledgements

Graduate school has been a long and trying adventure, and I would never have made it to the end if not the a host of people who rallied around me and guided me to the finish. First and foremost, I need to express my tremendous appreciation for my beautiful wife, Jessica. You have put up with a lot, and you have been my support group and cheerleader through it all. We have hit a lot of milestones these last few years, and I count myself very blessed to have done it all with you. Since I began this endeavor, we got married, you moved to Minnesota, we had a baby, and a lot more, and I look forward to continuing on to new and better things with you.

I am also grateful to my daughter, Lily, whose babbling and goofiness are always welcome after a hard day. Even when you have deprived me of sleep or a little peace and quiet, I have never been able to watch you and not smile.

My parents and brother have also always been everything that one could ask for in a family. I have always found it amusing that the son of two English teachers would be so driven away from the humanities and into the hard sciences, but I guess you managed to raise an academic one way or the other. Kevin, I thoroughly believe that I have you to thank for keeping me grounded in the real world. I would never have had the experiences and knowledge that I do if you hadn't been there to share them. Your methods might have been a bit unorthodox at times—like when you put a baseball glove on me and threw a tennis ball at my face to teach me to catch—but they worked.

Of course, I am deeply indebted to my advisor, Dr. Evan Skillman. Without your advice and guidance, I absolutely would not have succeeded. I can only imagine how frustrating I must have been at times, but I am all the more grateful that you were willing to teach me and stick with me through these five years. Your patience, good humor, and support have been invaluable throughout this process, and I can't thank

you enough.

I have had the great pleasure to work with many excellent scientists in my time at the University of Minnesota. In particular, I would like to thank Dan Weisz, whose interesting project ideas and willingness to teach gave me something to do and the knowledge to do it. I am also tremendously grateful to Kristy McQuinn. We have spent many hours talking about all things scientific and unscientific, and I am so thankful you have been willing to share you experience and wisdom with me. I also owe a great deal of thanks to Andy Dolphin for his willingness to share his tools and extensive know-how, without which I might never have finished.

To all my officemates, Jake, Jennifer, Ted, Steve, Danielle, Micaela, and Zahra, thank you for putting up with me and being a sounding board for all these years (especially Jake who had to share an office with me for five years!). I also need to thank the other graduate students who have helped me along the way. Without your knowledge-sharing and camaraderie, I never would have made it.

Finally, I thank the entire Minnesota Institute for Astrophysics faculty and staff, especially Terry Thibeault and Corinne Komor, without whom this department would surely break down into chaos. I acknowledge the support provided to me by Russ Penrose, whose generous fellowship allowed me to focus on my own research and helped me complete my degree.

Dedication

For my family.

Abstract

The star formation histories (SFHs) of galaxies can tell us a great deal about the formation and evolution of galactic systems. By creating color-magnitude diagrams (CMDs) of resolved stellar populations, we can derive the star formation rate (SFR) as a function of time and metallicity (i.e., the SFH) for the observed stellar population. In this thesis, I study the methods used to make these measurements and calculations, and apply them to conduct a study of the Magellanic Clouds. Throughout this study, we aim to address two fundamental questions: "How can we obtain deep, spatially comprehensive photometric coverage of dwarf galaxies and use those data to construct accurate and meaningful SFHs?" and "Can we constrain the possible evolutionary scenarios of the Magellanic Clouds from their ancient SFHs?"

We present the results from a study of the ancient star formation histories (SFHs) of the Large Magellanic Cloud (LMC) and the Small Magellanic Cloud (SMC). At about 50 kpc and 60 kpc away, respectively, from the Milky Way (MW), the LMC and SMC provide us an excellent opportunity to make deep photometric measurement, allowing us to construct an accurate ancient SFH. Using archival data from the *Hubble Space Telescope*/Wide Field Planetary Camera 2 (*HST*/WFPC2), we construct CMDs for 56 LMC fields and 15 SMC fields. This data set provides diverse spatial coverage as well as photometric depth that reaches well below the oldest main sequence turn off (MSTO), allowing us to construct a global SFH of each galaxy with excellent temporal resolution, even in the oldest time bins. We derive the SFHs using the same maximum likelihood CMD fitting technique for both the LMC and the SMC to allow for the direct comparison of the results, without the introduction of unnecessary systematic offsets and uncertainties. At very early times, we find that the LMC experienced an initial burst of star formation activity that was absent in the SMC. After about 12 Gyr ago, the SFHs both galaxies tracked each other very well. After about 12 Gyr ago, they were both relatively quiescent until 4–6 Gyr ago, when the star formation rate (SFR) dramatically increased in both galaxies, and maintained that rate until the present. These findings have driven us to conclude that the MCs did not originally form together, and they are likely on their first passage through the MW.

Finally, we discuss ongoing and upcoming studies of dwarf galaxies in the Andromeda system. Using ground-based and space-based data, we hope to derive spatially comprehensive SFHs with excellent temporal resolution. Accurate, quantitative SFHs of many of the Andromeda dwarfs will allow us to study a more significant portion of a whole galactic system than ever before. It will also have significant cosmological implications because we will be able to determine if the MW population is representative of galaxies in general or if the local environment plays a significant role in the evolution of a large galaxy.

Contents

List of Tables

List of Figures

Chapter 1

Introduction

Dwarf galaxies are the smallest, most common galaxies in the Universe (e.g., Marzke & da Costa, 1997). They are defined by their small size but should not necessarily be considered a unique class of system Tolstoy et al. (2009). The ability to consider dwarf galaxies as similar to other larger galaxies makes them objects of great interest. They are simpler than large galaxies, which allows for more thorough and complete study with more robust conclusions about their histories and properties. In hierarchical models of galaxy formation (e.g., Searle & Zinn, 1978), galaxies grow through the continual accretion of smaller galaxies or "protogalactic fragments." Evidence for this model grows as more and more evidence of past and ongoing interactions between dwarf galaxies and their neighbors is discovered (e.g., Mateo, 1998). By examining the structure of these small dwarf galaxies and reconstructing SFHs, we can get a glimpse of the construction of what will become the building blocks of larger galaxies.

There are two major types of dwarf galaxies, dwarf irregulars and dwarf spheroidals. It is likely that dwarf irregular galaxies evolve into dwarf spheroidals, but there are a few key differences between the two types that need to be reconciled for that idea to hold. Irregulars contain significant amounts of gas, have ongoing star formation, and are likely rotationally supported. Spheroidals, on the other hand, have no gas or ongoing star formation and are pressure supported. For the proposed evolution to take place, gas must be expelled, thereby preventing further star formation, and angular momentum must removed to evolve from rotational support to pressure support.

Another important difference between the types of dwarfs is their spatial distribution. Irregulars are found preferentially isolated, far away from large galaxies (e.g., Grebel, 1999; James & Ivory, 2011). Spheroidals, however, are most often found near a large host galaxy like Andromeda or the Milky Way. This relationship between distance and morphology implies that proximity to a large galaxy likely plays some role in the evolution from dIrr to dSph.

At first it seems difficult for a galaxy to dramatically change its angular momentum and change from rotationally supported to pressure supported, but simulations show it is not only possible but likely (Mayer et al., 2006). Beginning with a dIrr orbiting in the external potential of a galaxy like the Milky Way, they find dramatic morphological changes after only $2-3$ pericenter passages. On the first passage, the satellite galaxy develops a central bar. The bar's rotation slows and angular momentum is lost to dynamical friction. At the same time, the material farthest out in the bar (with the most angular momentum) is stripped. Soon after the first orbit, the bar begins to buckle. The buckling and the induced vertical heating lead to a more spherical geometry. After ~ 7 Gyr, nearly all the objects studied had been transformed into spheroidals.

Interestingly, the light profile of a galaxy undergoing such transformation will not change dramatically. The profiles of dIrrs are often fit using exponential functions. Dwarf spheroidals are usually fit using King profiles, but they are also quite well-fit with exponential profiles. King profiles naturally fit slightly better because of the extra free parameter. Simulations have shown that a significant mass loss event–which is necessary for evolution from irregular to spheroidal–will naturally leave a stellar component that is well-fit with an exponential profile (e.g., Read & Gilmore, 2005).

This thesis focuses primarily on two dwarf galaxies in the Milky Way system: the Large Magellanic Cloud (LMC) and the Small Magellanic Cloud (SMC). The Magellanic Clouds make interesting targets because, contrary to the distance-morphology relation mentioned above, they are dwarf irregular galaxies, relatively close to the Milky Way at distances of ~ 50 kpc for the LMC and ~ 60 kpc for the SMC. They are also two of the best studied galaxies in the Universe (e.g., Zaritsky et al., 1997; Kim et al., 1998; Zaritsky et al., 2002; Stanimirović et al., 2004; Kallivayalil et al., 2006a,b; Meixner et al., 2006, 2010; Udalski et al., 2008a,b; Kerber et al., 2009; Gordon et al., 2011; Rubele et al., 2012). Despite that fact, relatively little is known about their ancient star formation

histories. In this work, we utilize archival data from the *Hubble Space Telescope*/Wide Field Planetary Camera 2 to remedy that shortcoming and achieve three major goals:

- Derive accurate ancient SFHs for fields in the LMC and SMC
- Combine SFHs of individual fields into approximate global SFHs for each galaxy
- Constrain evolutionary scenarios of the LMC and SMC

The organization of this thesis is as follows. The main body of the work will be presented in Chapter 2. It is here that I discuss our project to derive the ancient SFHs of the Magellanic Clouds. I was personally responsible for retrieving and sorting the archival data to obtain the data set that is best suited to the goals of the study, as well as performing the analysis. In Chapter 3, I will briefly discuss ongoing and future efforts to expand the work of this thesis. I will focus on an ongoing study of the Andromeda system, in which we conduct similar analysis using ground-based data. I summarize the main results of my work in Chapter 4.

Chapter 2

The Ancient Star Formation Histories of the Magellanic Clouds[1]

We present the results from a study of the ancient star formation histories (SFHs) of the Large Magellanic Cloud (LMC) and the Small Magellanic Cloud (SMC). After examining 101 archival *Hubble Space Telescope*/Wide Field Planetary Camera 2 (*HST*/WFPC2) fields in the LMC and 28 fields in the SMC for adequate depth of photometry, we construct color-magnitude diagrams (CMDs) for 56 LMC fields and 15 SMC fields. The photometry from these 71 spatially diverse fields reaches > 2 magnitudes below the oldest main sequence turn off (MSTO), even in high surface brightness regions near the centers of the galaxies, where ground-based studies are typically crowding limited. Our deep photometry and large sample allow us to study the ancient (> 4 Gyr) SFHs of the Magellanic Clouds (MCs) in unprecedented detail. We derive the SFHs using the same maximum likelihood CMD fitting technique for both galaxies to allow for direct comparison and minimize systematic uncertainties. We then sum the SFHs of the individual

[1] **Based on observations made with the NASA/ESA Hubble Space Telescope, obtained at the Space Telescope Science Institute, which is operated by the Association of Universities for Research in Astronomy, Inc., under NASA contract NAS 5-26555**

fields to derive the approximate global SFH of each galaxy. From the global SFHs, we find that the LMC experienced a significant initial burst of star formation 12–14 Gyr ago, forming over 20% of its mass before 12 Gyr ago. The SMC lacks a similar burst of early star formation, forming only 20% of its stellar mass during its first ∼9 Gyr. This implies a suppression or underfuelling of ancient star formation in the SMC. The difference between the two SFHs may be due to their different masses, but also suggests that the MCs probably did not form as a bound pair. We do not see any periodic features in the SFH of either galaxy, suggesting that repeated encounters with the Milky Way are unlikely. Beginning 4–6 Gyr ago, both galaxies show a significant increase in SFR. Subsequently, both SFHs track each other quite closely. We do not notice any significant spatial gradients in either galaxy.

2.1 Introduction

Because of their close proximity, the Large Magellanic Cloud and the Small Magellanic Cloud are two of the most frequently and thoroughly studied galaxies in the Universe. Despite the large number of studies devoted to understanding the Magellanic Clouds, their origins remain somewhat mysterious. It is unclear whether these galaxies formed together or separately, and determining how long they have been satellites of the Milky Way (MW) has been the subject of many investigations. It had long been believed that the MCs are in bound orbits around the MW, and the observed tidal features (e.g., the Magellanic Stream) are the result of successive MW encounters (e.g., Murai & Fujimoto, 1980; Gardiner & Noguchi, 1996; Yoshizawa & Noguchi, 2003; Connors et al., 2006). However, HST-based proper motion studies (Kallivayalil et al., 2006a,b, 2013) and new 3D velocities suggest bound orbits posited by traditional models are implausible (Besla et al., 2007; Boylan-Kolchin et al., 2011; Busha et al., 2011). Even their location in the MW system has raised questions because studies find that it is rare to find star forming dwarf galaxies so close to a large host (e.g., Grebel, 1999; James & Ivory, 2011). Tollerud et al. (2011) found that MW analog galaxies in ΛCDM simulations have satellites comparable to the LMC within 75 kpc with a frequency of only ∼10%.

Even their location in the MW system raises questions because studies find that it is rare to find star forming dwarf galaxies so close to a large host (e.g., Grebel, 1999; James & Ivory, 2011).

One key to understanding the origins of the MCs lies in their ancient stellar populations. Tidal encounters between galaxies are known to induce elevated levels of star formation, leaving signatures of past interactions in the stellar fossil record of each galaxy (e.g., Besla et al., 2007, 2012). By constraining the ancient SFHs of the MCs, and matching past patterns of star formation to interaction timings predicted from dynamical models, we can begin to discriminate between likely and unlikely evolutionary scenarios.

Despite a large number of studies devoted to understanding the MCs and their SFHs, surprisingly little is known about their ancient ($>$ 4 Gyr ago) SFHs. Space-based observations with instruments like the *HST* are excellent tools for obtaining deep photometry, easily capable of seeing down to the oldest main sequence turn-off (MSTO) and beyond, but they are lacking in their field of view (e.g., Geha et al., 1998; Holtzman et al., 1999; Olsen, 1999; Dolphin et al., 2001; Cignoni et al., 2012). These studies have been able to constrain the SFHs at all ages, but general conclusions about the ancient SFHs of the MCs from these studies are somewhat limited due to the small spatial areas sampled.

Conversely, ground-based observations are much more capable of providing comprehensive coverage, but they are unable to provide the depth of photometry necessary to study the ancient SFHs of the MCs. In fact, because the MCs are so close, ground-based observations are capable of reaching photometric depths below the oldest MSTO, but only in the uncrowded, outer regions of the galaxies (Zaritsky et al., 2002, 2004; Harris & Zaritsky, 2004, 2009; Udalski et al., 2008a,b; Kerber et al., 2009; Noël et al., 2009; Saha et al., 2010; Piatti et al., 2012; Rubele et al., 2012). Near the centers of the galaxies, the stellar density is too high to allow ground-based instruments to make accurate photometric measurements.

Additionally, studies often focus on either the LMC or the SMC, using different analysis techniques for each. The lack of consistent methods for measuring the SFHs introduces systematic offsets that can be very difficult if not impossible to reconcile, making a direct comparison of the SFHs of the two galaxies very difficult.

We attempt to remedy these shortcomings by utilizing archival *HST*/Wide Field Planetary Camera 2 (WFPC2) data. Our sample covers a large, representative area of each galaxy, giving us the benefit of a large field of view, like that provided by ground-based instruments. Our use of *HST*/WFPC2 provides photometry that is significantly deeper than the oldest MSTO, even in the crowded, central regions of the galaxy, allowing us to study the ancient SFH throughout both of the galaxies. We also conduct analysis using the same maximum likelihood fitting technique for both galaxies, allowing for direct comparison of their SFHs.

In Weisz et al. (2013), we demonstrated the quality of the data and calculated the SFHs of 7 of our 15 SMC fields and 8 of our 56 LMC fields. We also provided preliminary global SFHs calculated for each the LMC and SMC and briefly commented on the implications of those results on evolutionary scenarios of the MCs. Now, we aim to expand on that previous work and provide more robust global SFHs, utilizing significantly more data.

In this chapter, we present SFHs for 56 LMC fields and 15 SMC fields observed with *HST*/WFPC2 as well as global SFHs for the LMC and SMC. We discuss the origins of our data and present CMDs in Section 2.2. In Section 2.3, we discuss our method for measuring SFHs. We present the derived SFHs for each field in Section 2.4 and global SFHs for each galaxy in Section 2.5. In Section 2.6 we examine spatially resolved features of the LMC, in Section 2.7 we compare our SFHs to those of MC clusters, and in Section 2.8 we discuss the implications of our work for evolutionary scenarios for the MCs. Finally, Section 2.9 summarizes the work.

2.2 The Data

For this study, we use photometry and artificial star tests (ASTs) from the Local Group Stellar Photometry Archive[2] (LOGPHOT; Holtzman et al., 2006). LOGPHOT houses data for several hundred fields in both the LMC and SMC from which we have carefully selected our sample. Because of their large angular size, it would take tens of thousands of pointings for *HST* to cover the LMC and SMC completely; therefore, we have taken advantage of archival data in LOGPHOT to achieve the best coverage possible. Figures

[2] http://astronomy.nmsu.edu/logphot

2.1 and 2.2 show the positions of all the fields used and demonstrate that our sample covers representative regions of both galaxies, including central, disk, and halo fields.

The LMC dataset was selected exclusively from the Priority 1 fields in LOGPHOT. Priority 1 fields have the highest quality data and typically include deep exposures in F555W and F814W. Fields were chosen to avoid clusters and diffuse emission, especially in regions near Supernova 1987a. This study is focused on determining the SFH of the field populations in the MCs, so fields containing clusters were excluded to avoid contamination. After these exclusions, we were left with 56 fields, covering a wide area of the LMC.

Of the nine Priority 1 fields in the LMC, two of them were excluded because they contain clusters. Of the remaining seven, four of them (u37704, u377a4, u37706, u377a6) are so close together and sparsely populated that they were combined into one, essentially yielding only four Priority 1 fields in the SMC. Therefore, we decided to include Priority 2 fields in our SMC sample.

Priority 2 fields were chosen based on the availability of high quality F606W and F814W photometry. (F555W photometry is not available for Priority 2 fields.) Similar to the LMC, diffuse emission and clusters were avoided. Unlike our Priority 1 sample, Priority 2 fields were often saturated and had to be selected so that important CMD features were still sampled. After carefully selecting only the best Priority 2 fields, we were able to add eight more fields to our SMC sample.

While we considered adding Priority 2 fields to our LMC sample to preserve the consistency of analysis between the two galaxies, such additions were judged to add very little to the results. Both Priority 1 and Priority 2 fields are analyzed using identical techniques. The only difference is the presence of the F606W filter in the Priority 2 data in place of F555W, so we believe that consistency is conserved.

For each individual field, we have only considered objects detected with a signal-to-noise ratio (SNR) ≥ 10 in both of the desired filters. Objects that are not consistent with point sources, such as elongated objects and objects whose light profiles are too sharp, are also discarded. The SNR information for each filter and other detection quality values are encoded in a bit flag in LOGPHOT (See Table 2 in Holtzman et al. (2006)). Our desired quality characteristics correspond to FLAG ≤ 1 if only our two filters of interest are available. If other filters are also present in the photometric

reduction, we ignore their data quality by allowing bits corresponding to those unwanted filters indicating low SNR to be set. This filtering process yields the maximum number of objects while maintaining our strict detection quality requirements.

We also utilize artificial star tests (ASTs; $> 10^5$ per field) available in LOGPHOT to characterize the completeness of the photometry in each field. ASTs were filtered in exactly the same way as the photometry. Those objects that were not recovered with sufficient SNR in a particular filter were labelled unrecovered only in that filter, and objects that failed to meet one or more of the other global quality criteria were marked as unrecovered in both filters.

We have plotted the CMDs of all the LMC and SMC fields in Figures 2.3 and 2.4, respectively. Critical age-sensitive features like the oldest MSTO, subgiant branch, and red giant branch (RGB) are present in all our CMDs and are thoroughly sampled in many, though the RGB is truncated in some of the Priority 2 fields because of saturation. The ability to see these features, especially the oldest MSTO, provides confidence in our determinations. For both galaxies, our *HST*-based CMDs are $\gtrsim$ 2 magnitudes deeper than CMDs from current ground-based observations. The data are also highly complete down to their limiting magnitudes, given in Table 2.1.

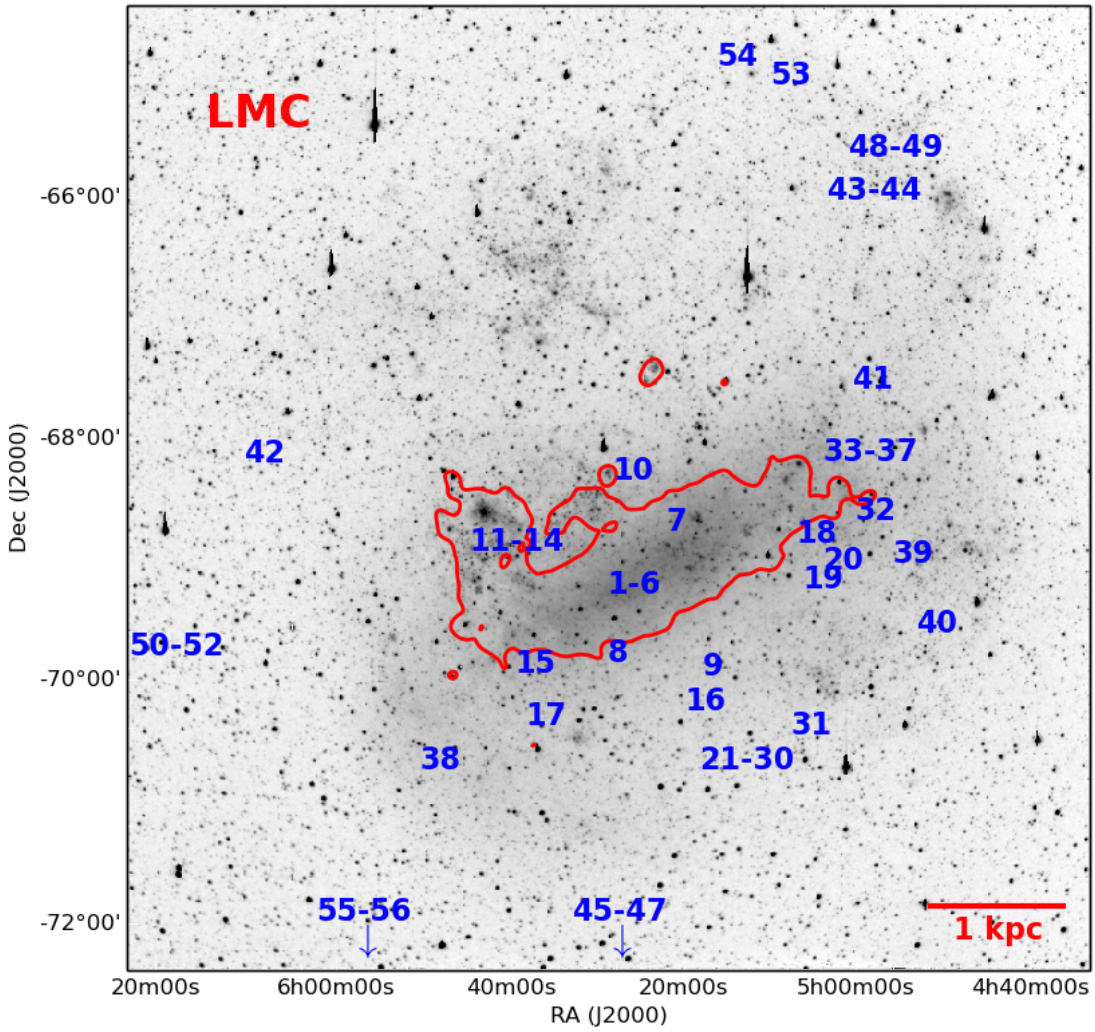

Figure 2.1: A map of the LMC showing the spatial locations of the *HST*/WFPC2 fields used in this study. For this study, the LMC bar was defined to be inside the red contour, which represents $F_{4.5\mu m} > 0.3$ MJy/str (Meixner et al., 2010). The fields are numbered according to galactocentric radius, though fields that are very close together were always labelled with consecutive numbers. (Background image: Bothun & Thompson, 1988)

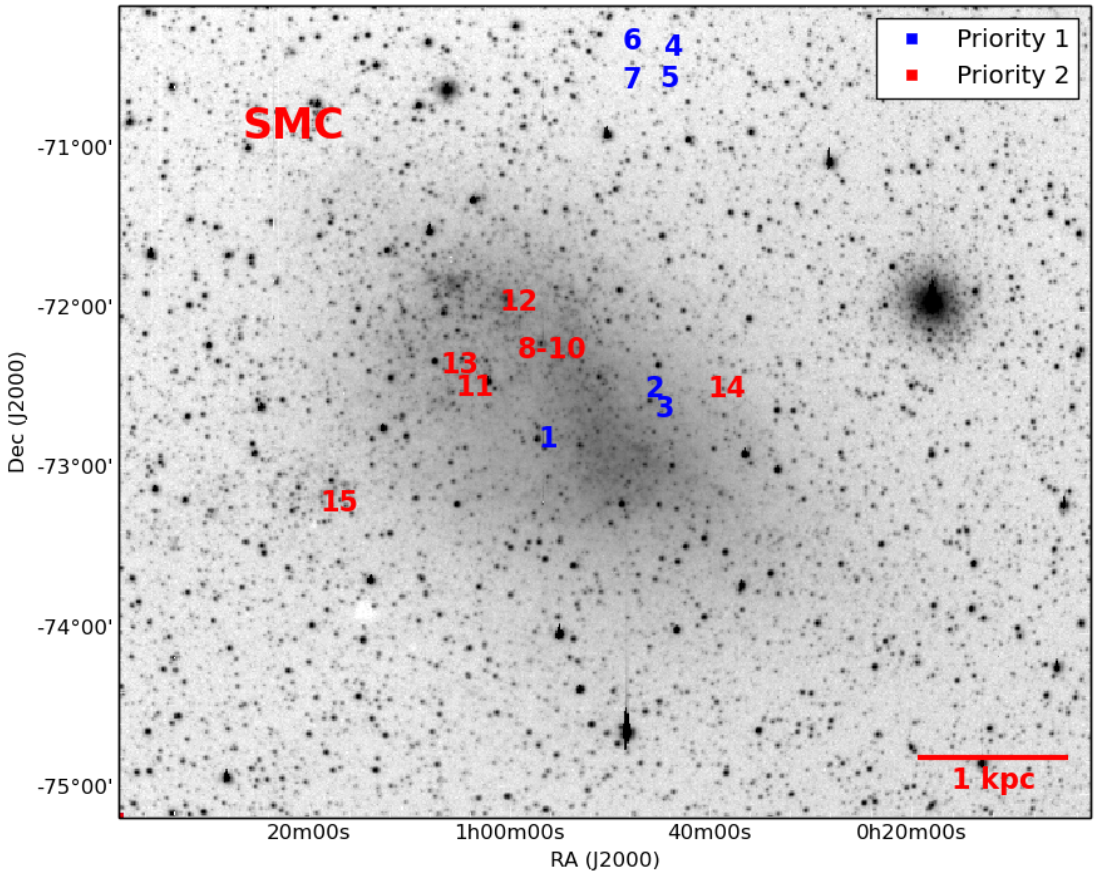

Figure 2.2: A map of the SMC showing the spatial locations of the *HST*/WFPC2 fields used in this study. The fields are numbered according to galactocentric radius. (Background image: Bothun & Thompson, 1988)

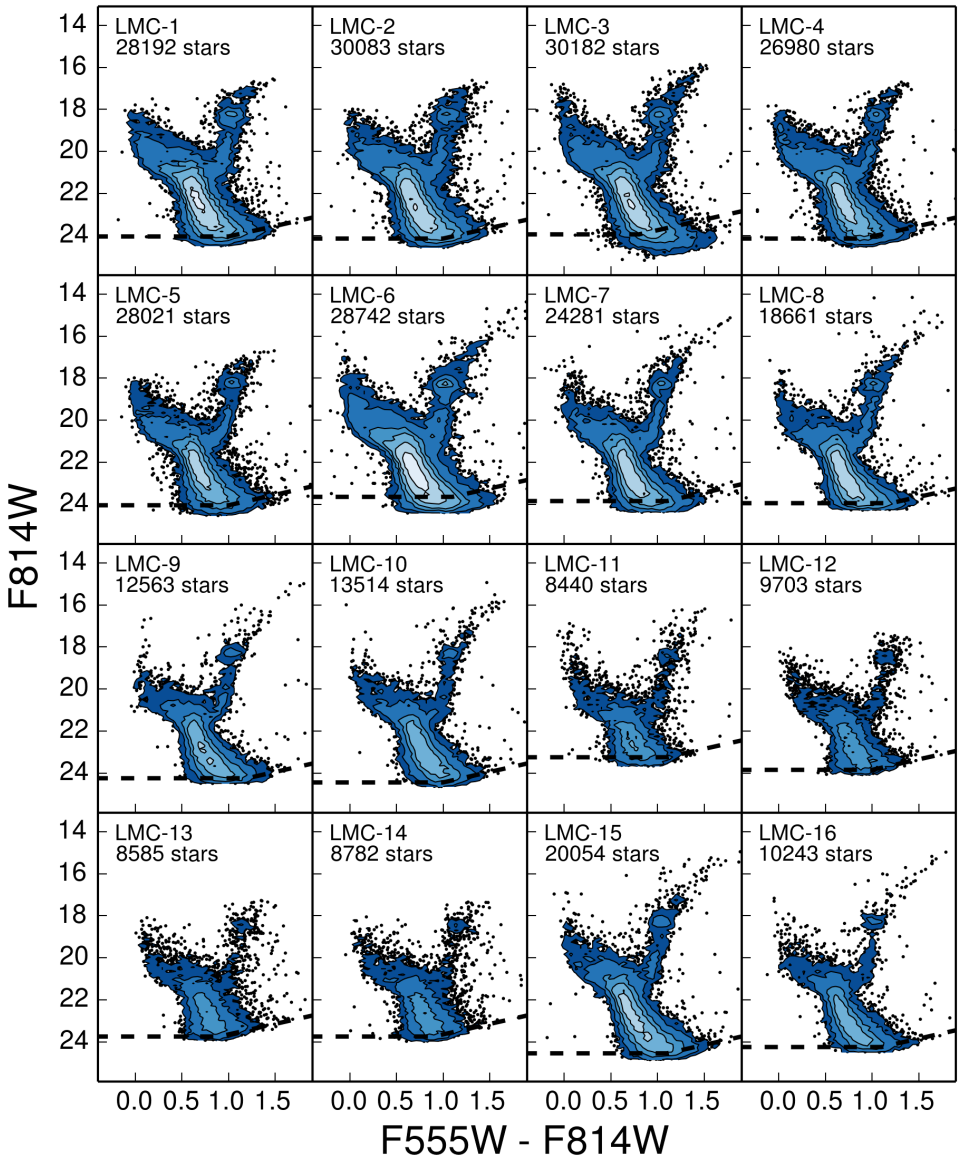

Figure 2.3: *HST*/WFPC2-based CMDs of the 56 LMC fields in our sample. The stellar density contours range from 2 (dark blue) to 512 (white) stars decimag^{-2}. These CMDs contain all the stars in their respective fields detected with SNR $\geq$ 10 in for F555W and F814W. The 70% completeness limits are denoted by the black dashed line. Other CMD characteristics are listed in Table 2.1. These CMDs reach $>$ 2 magnitudes deeper than the oldest MSTO, even in central regions of the galaxy where stellar densities are high and ground based studies are often crowding limited.

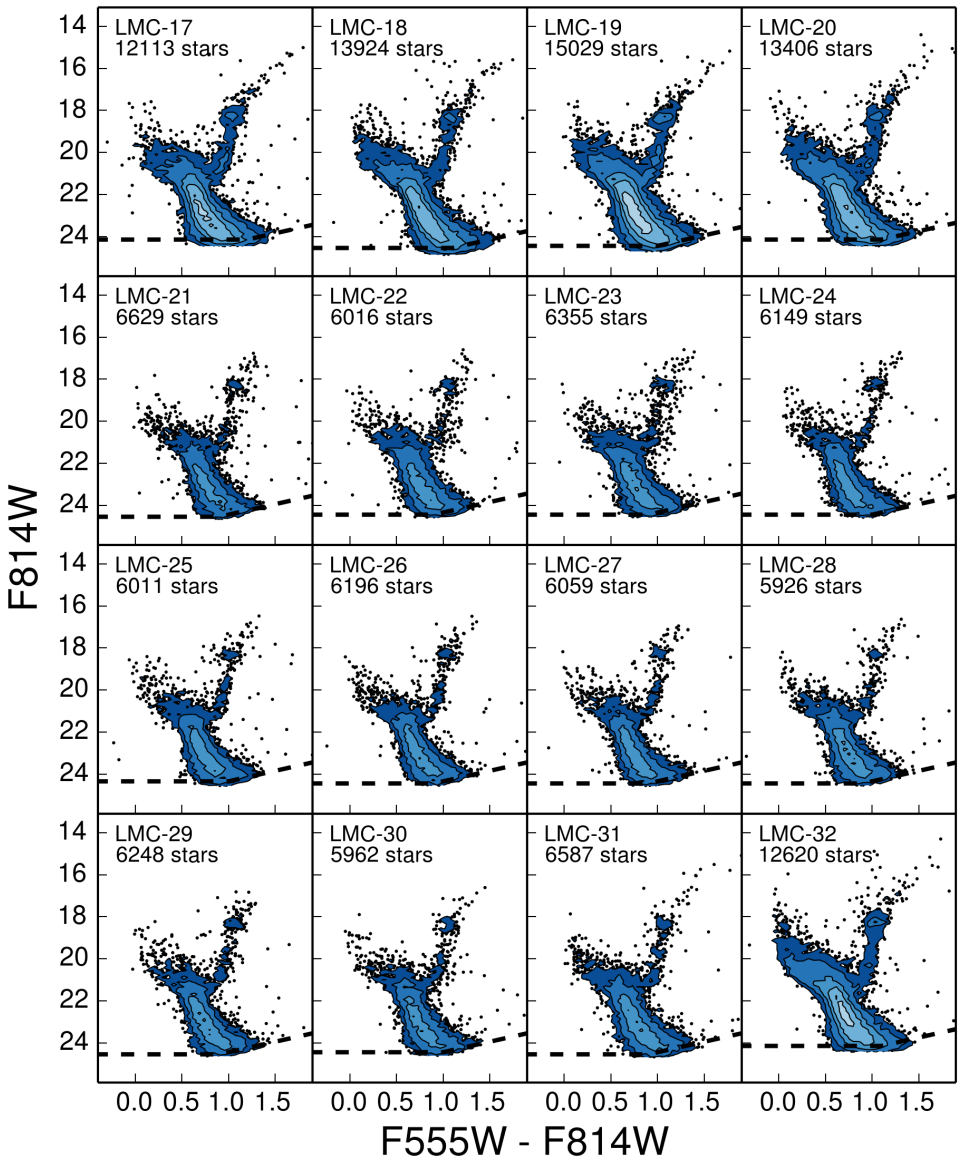

Figure 2.3: cont'd

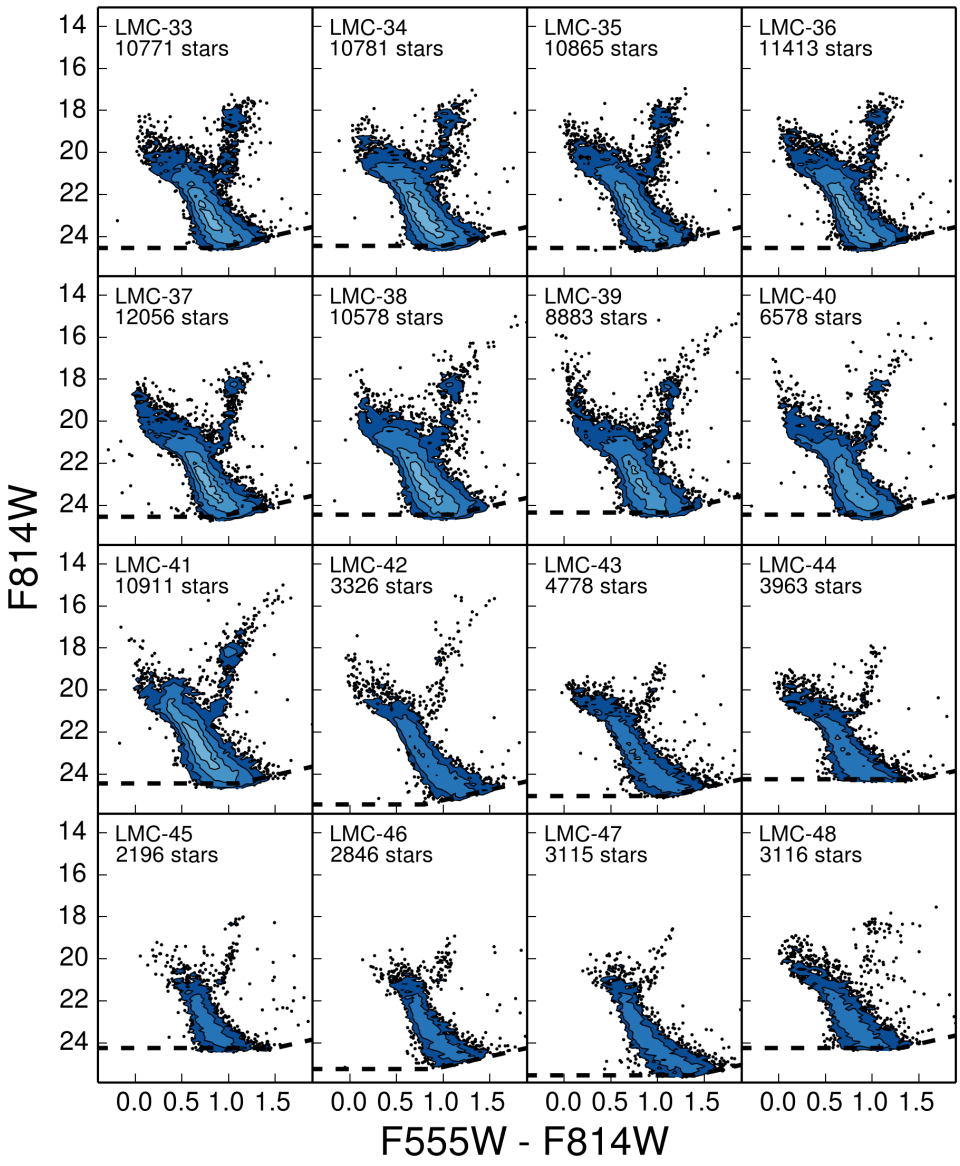

Figure 2.3: cont'd

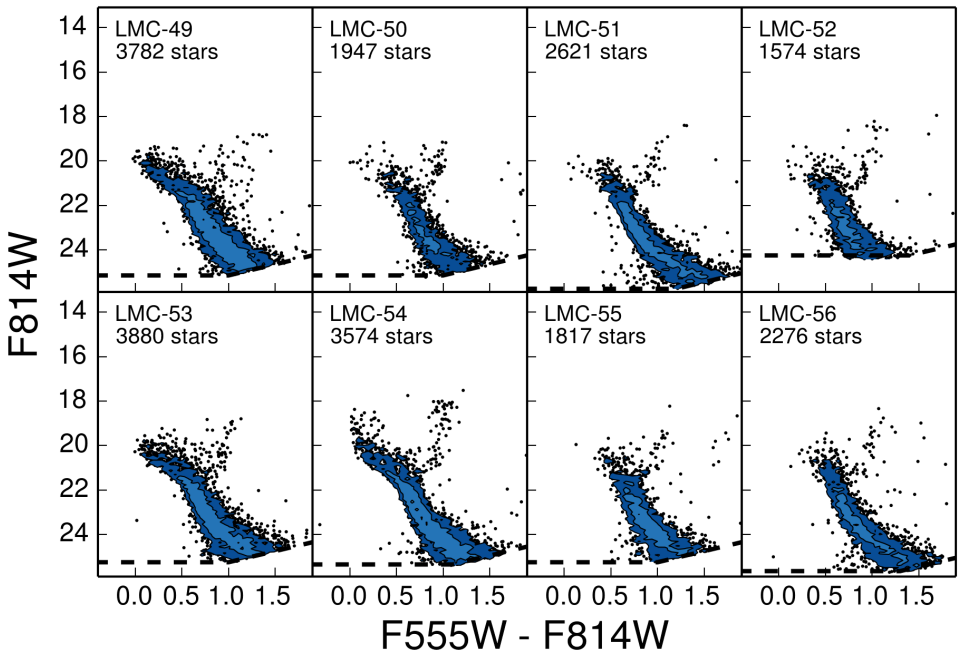

Figure 2.3: cont'd

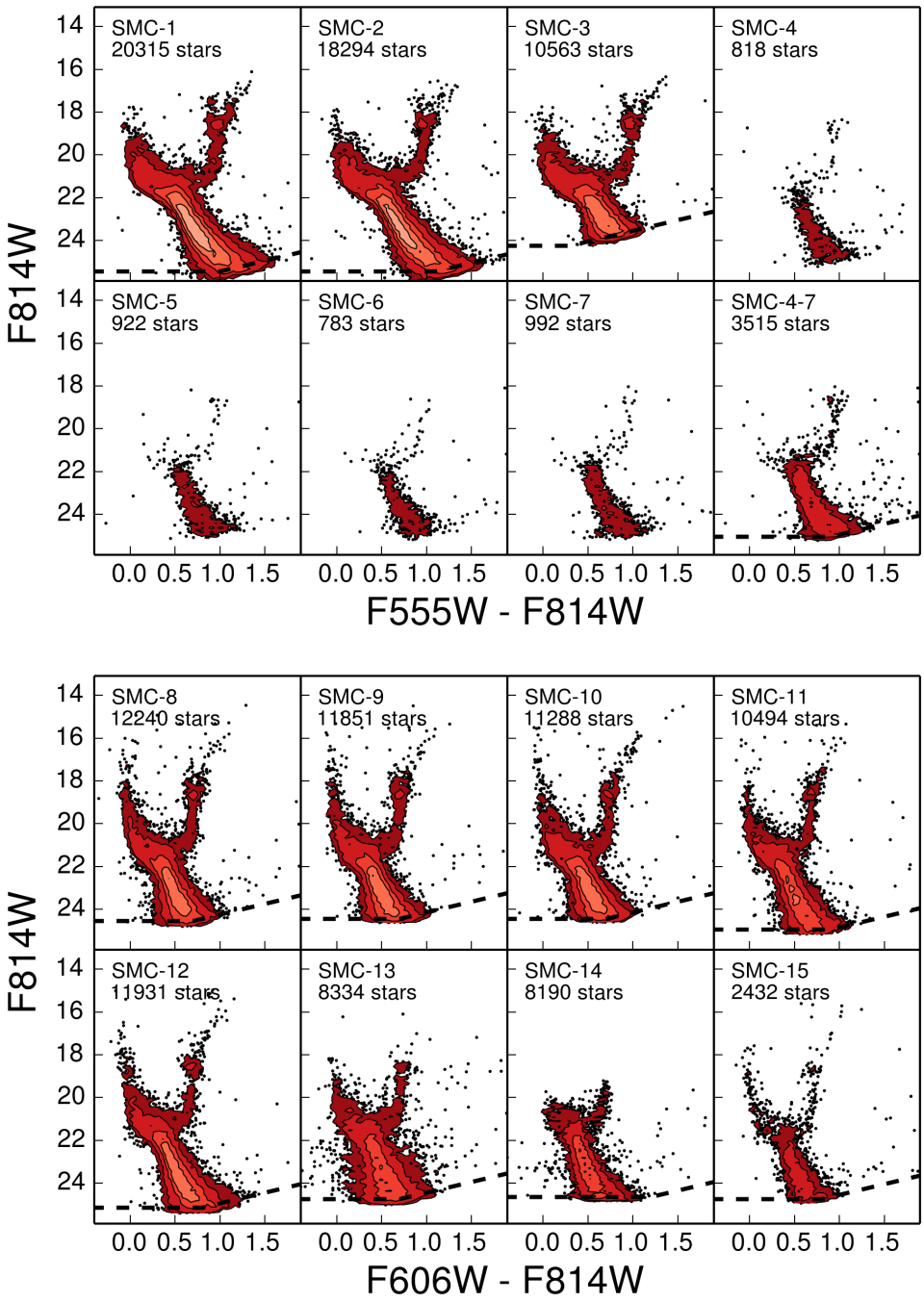

Figure 2.4: *HST*/WFPC2-based CMDs of the 7 Priority 1 fields (top) and 8 Priority 2 fields (bottom) for the SMC. The stellar density contours range from 2 (dark red) to 512 (white) stars decimag^{-2}. The Priority 1 fields use the F555W and F814W filters on WFPC2, and the Priority 2 fields use the F606W and F814W filters because no F555W data were available. In both cases, the CMDs reach $>$ 2 magnitudes deeper than the oldest MSTO, even in central regions of the galaxy where stellar densities are high and ground based studies are often crowding limited. The 70% completeness limits are denoted by the black dashed line. Other CMD characteristics are listed in Table 2.1.

2.3 Measuring the Star Formation Histories

Using the photometric catalogs and ASTs from LOGPHOT, we measured the SFH of each field using MATCH(Dolphin, 2002). Using a set of input parameters (stellar models, initial mass function, binary fraction) MATCH constructs a set of synthetic simple stellar populations (SSPs) over specified ranges in age and metallicity. For this study, we used stellar models from Marigo et al. (2008) and Girardi et al. (2010), a Kroupa (2001) initial mass function (IMF), with mass limits ranging from 0.15 to 120 $M_{\odot}$, and a binary fraction of 0.35. Using a maximum likelihood technique, MATCH weights and linearly combines the synthetic SSPs and convolves them with observational errors calculated from analysis of the ASTs to generate synthetic CMDs until a best match to the data is found. The SFH of the best fit composite synthetic CMD is the most probable SFH of the observed CMD. This process is repeated for various values of distance and reddening, so most likely values for those free parameters are found as well. A more detailed description of MATCH can be found in Dolphin (2002).

2.3.1 Distance and Reddening

While searching for the most likely SFH of the observed CMD, MATCH also solves for the most likely distance modulus and reddening value. A range and step size for each is input into MATCH, which then varies the distance and extinction according to the input, along with the SSPs, to generate a synthetic CMD that is the best fit to the observed data.

For our study, we restricted extinction to be $0.0 \leq A_V \leq 0.3$, and searched in that range with a step size of 0.05 dex. Initially, we fixed the distance modulus for each field to be 18.45 for the LMC and 18.90 for the SMC (Bono et al., 2008; Dolphin et al., 2001, respectively) to simplify our analysis and maintain consistency; however, such strict constraints under-fit the data. For many fields, the resulting solution created a significant residual between the observed and modelled CMD.

To correct the residual, we allowed MATCH to treat distance modulus as a free parameter and search for the best fit within a range of 18.30–18.60 for the LMC and 18.75–19.05 for the SMC. All of the fields found high-quality fits within those ranges, as can be seen in Table 2.1.

2.3.2 Differential Extinction

Many of the fields in our sample show evidence of significant differential extinction. Differential extinction occurs when lines of sight to some stars contain more dust than others (e.g., looking at stars in front of and behind the disk of a galaxy). It manifests itself as the stretching of the CMD features (e.g., the red clump) along the reddening vector. For example, the CMD of LMC-19 (2.3) clearly shows an elongated red clump, which is caused by differential extinction along the line of sight to that field.

We consider differential extinction for all fields even though not all are significantly affected. Doing so not only maintains the consistency of our analysis, it also ensures that MATCH is not just using differential extinction as an additional free parameter. Upon cursory inspection of the CMD, it is easy to see if a field requires significant differential extinction or not. For a field with little or no differential extinction, a solution containing a significant amount does not make physical sense. If MATCH returns such solutions, adjustments clearly need to be made.

The stellar models of Marigo et al. (2008) and Girardi et al. (2010) do an excellent job matching bright features like the RGB and asymptotic giant branch (AGB), but they do not fit the lower main sequence (MS) in our data as precisely. Specifically, the lower MS features in the models are not as broad as the observed MS, possibly due to underestimated photometric uncertainties. This issue often forced MATCH to try to use too much differential extinction to artificially broaden the lower MS of the synthetic CMD to match the observations, even on fields that do not require significant differential extinction.

To minimize the affect this problem, we use shallower photometry, with a cut-off point of $M = 22.2$ in the bluer filter (versus $M = 23.5$ used in the rest of this study) when fitting the differential extinction. The shallower photometry does not include the lower MS, allowing differential extinction to be determined based only on the appropriate CMD features, like the red clump and RGB. Our final SFHs were then calculated by utilizing our deeper photometry ($M \leq 23.5$) and the differential extinction value found using this method.

2.3.3 Constraints on the Age-Metallicity Relationship

When measuring the SFH of a field, MATCH also solves for the age-metallicity relationship (AMR). While this information provides useful insight into the environment in which the stars in that field formed, there can be a degeneracy between metallicity and extinction. To prevent this degeneracy from affecting our results, we used 23 fields that did not appear to have significant differential extinction to solve for an average AMR for each galaxy, and then applied that AMR to all the fields in its respective galaxy. By using well-sampled fields that do not show evidence of differential extinction, we allowed MATCH to solve for initial and final metallicities. We also found the best AMR for the galaxy by allowing MATCH to consider three options: an AMR that is linear with $\log(Z)$, an AMR that is linear with Z, and an AMR that has the most enrichment early on in the galaxy's history. By using fields with very little differential extinction, we were able to break the degeneracy and find a reasonable AMR by searching over these parameters and finding the best fit. We then adopted a single AMR for all the fields in each galaxy when solving for the SFH.

The derived SFH does not change dramatically in spite of significant changes to the AMR, so even though it is possible that the AMRs vary slightly from field to field, our results will not be greatly affected. Also, by defining the parameters of the AMR as reasonable quantities, we can be sure that our resulting SFHs make physical sense as well.

2.4 Star Formation History Solutions

Once we have defined all the proper constraints, MATCH is able to generate a solution for the most likely SFH for each field. It is fairly easy to determine if the solution is a good fit by examining the residual difference between the observed and modelled CMD. Figure 2.5 shows a typical example of the fits MATCH generates for our data, as well as the resulting SFH. As discussed in Section 2.3, the modelled CMD is created from a linear combination of SSPs generated from stellar models. The lack of structure in the residual image shows that there are no systematic differences between the observed and modelled CMD, so the fit is good. From the combination of SSPs used to generate the modelled data, we can construct the most likely SFH for this field.

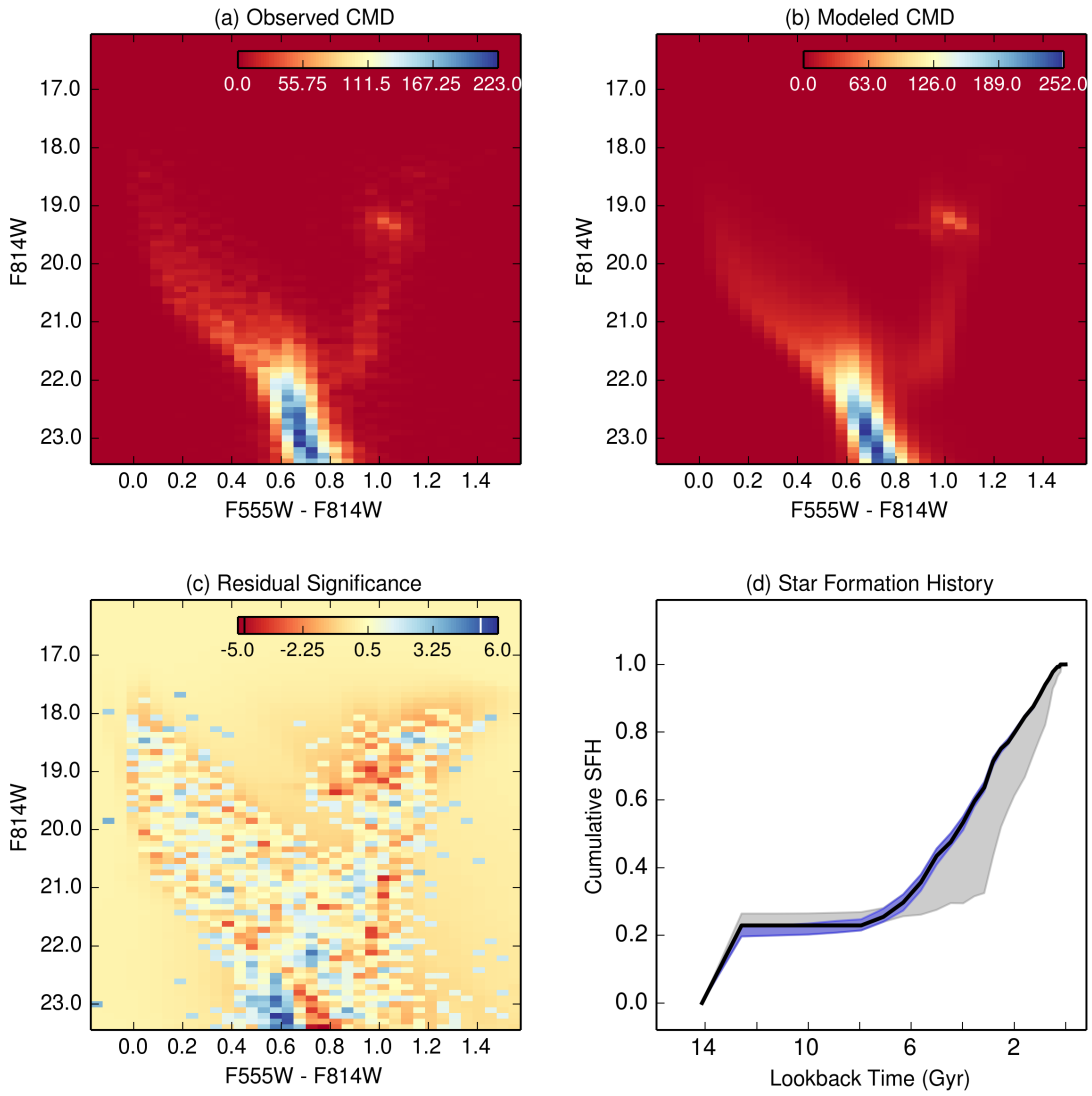

Figure 2.5: An example of the fit generated by MATCH for the LMC field u2c501 (LMC-54). Panel (a) shows the observed CMD. Panel(b) shows the best-fit modelled CMD generated by MATCH. Panel(c) shows the residual significance between the observed and modelled data. The residual significance illustrates the statistical significance of any residual. Panel (d) shows the cumulative SFH of the field. The blue shading represents the statistical uncertainties and the grey shading represents the total uncertainties, including both the statistical and estimated systematic uncertainties. We can see that this example is well fit because the residual significance is not large in any area, and there is no notable structure indicating a systematic difference between the observed and modelled data.

For all 71 fields, we have examined the fits created by MATCH and updated the input parameters as necessary to correct any systematic differences between the observed and modelled data until the two CMDs are a satisfactory match. The goodness of fit parameter that is used to determine the best fit is calculated using a Poisson maximum likelihood statistic, based on the Poisson equivalent of χ^2. Equation 2.1a gives the full formulation of the MATCH fit parameter, but for large-number statistics, it reduces to the expected χ^2 formalism, given by Equation 2.1b. More details are available in Dolphin (2002).

$$\text{fit} = 2\sum\left[m_i - n_i + n_i \times \ln\left(\frac{n_i}{m_i}\right)\right] \tag{2.1a}$$

$$\approx \sum \frac{(n_i - m_i)^2}{m_i} \text{ (for large-number statistics)} \tag{2.1b}$$

m_i = number of model points in bin i

m_i = number of observed points in bin i

The best fit is defined by the set of parameters that minimizes the MATCH fit parameter. When the best fit was found to reside at the upper or lower bound of the allowed range of any parameter, the range of that parameter was widened until a best fit was found to reside within the allowed parameter space. Once such a fit is found, we examine the residual of the observed and modelled CMD to ensure the goodness of the fit (e.g., see Figure 2.5). In all cases, when a best fit was found by MATCH that resided within the allowed parameter space, there was no significant residual between the two CMDs, so we can be confident in the resulting SFHs.

2.4.1 Error analysis

When estimating random uncertainties of star formation histories, bootstrap Monte Carlos are the standard technique. Unfortunately, this method systematically underestimates uncertainties in bins where star formation is low or zero. For this analysis, we implement the hybrid Monte Carlo (HMC) algorithm, as described in Dolphin (2013), and direct the reader to that paper for a detailed description of the implementation.

Systematic uncertainties are also estimated using the method outlined in Dolphin

(2012). This method estimates the effect of systematic uncertainties in the adopted isochrone set by modelling the isochrone differences as shifts in M_{bol} and $\log T_{eff}$. The shifts in M_{bol} and $\log T_{eff}$ are used as a proxy to reproduce the errors in age and metallicity for the SSPs that make up the observed population. We use MATCH to measure the SFH of each fields 50 times, using the input parameters that generated the best fit SFH for the field and shifts in M_{bol} and $\log T_{eff}$ (randomly chosen from Gaussian distributions with $\sigma_{\log T_{eff}} = 0.013$ and $\sigma_{M_{bol}} = 0.19$). The variation between these solutions is used to measure the systematic uncertainties. For a more detailed description of this method, please see Dolphin (2012).

For all of the panels in Figures 2.6 and 2.7, the black line represents the most likely SFH, the blue/red envelopes around the most likely SFH represent the random uncertainties, and the grey envelopes represent the total uncertainties, including both random and systematic. For points of reference, the dotted line is included to represent an average constant SFH, and the dashed line illustrates when 50% of the total stellar mass was formed.

The random uncertainties are always reasonably small, and most fields have very reasonable total uncertainties; however, there are a handful of fields in both the LMC and SMC for which the systematic uncertainties are relatively large. Most of these fields have such large errors because they contain a relatively small number of stars. Other fields—notably LMC-9 and LMC-33—likely have such large systematic uncertainties because they show high values of differential extinction. It is possible that significant differential extinction allows for varying SFH solutions because, depending on the stars to which the extinction is applied, once all the stars are extinction corrected, the CMD could appear to be the collection of a significantly different combination of SSPs, which would directly cause MATCH to infer a different SFH for the field. In all cases, our uncertainties illustrate how reliable our results are. In some cases, large systematic uncertainties serve to demonstrate just how challenging it is to derive accurate SFHs, even with excellent photometry.

To calculate the uncertainties for the combined SFHs (seen in Figures 2.8, 2.11, and 2.13), we used an approach that is very similar to that described above. Since we have used a sum to combine the SFHs of the individual fields in global SFHs, the random uncertainties are simply added in quadrature. To find the systematics, we again solve

for the SFH 50 times for each fields, but for each run (run01, run02, etc.) we initialize MATCH with the same random seed across all fields. This step ensures that the results from each run (run01, etc., for all fields) can be added together in the same way that we combined the best-fit SFHs to obtain a global SFH. The summed results for each of our 50 runs are then combined—just as described for an individual field—to give us the final systematic uncertainties of the global SFH.

2.4.2 Star formation histories of individual LMC fields

Figure 2.6 shows the SFH derived for each of our 56 LMC fields. A cursory inspection of Figure 2.6 reveals that the SFHs for the different fields can be roughly divided into three groups.

In the first group are those fields that show an initial burst of star formation activity followed by a period of relative quiescence. While it is interesting that the fields exhibiting this behavior are preferentially near the center of the galaxy, including fields 1–7 and 15, which are situated in or very near the LMC bar, it is also interesting that fields with a similar pattern of star formation are scattered throughout the galaxy.

These fields formed 20%–40% of their total stellar mass between 12 and 14 Gyr ago. Subsequently, they experienced little to no star formation activity until 6–8 Gyr ago. At that point, star formation resumed, and proceeded at a fairly constant rate until the present day.

Several of the fields in this group show the same initial burst followed by a period of quiescence, but resumed star formation earlier than 6–8 Gyr ago. Fields 20 and 26 are excellent examples of this behavior: they formed about 20% of their total stellar mass before 12 Gyr ago, and then star formation halted for a period of time. Similar to the group of fields mentioned above, they later resumed star formation, which continued at a relatively constant rate until present time, but unlike those fields, they resumed their star formation about 2 Gyr earlier, at $\sim$ 10 Gyr ago. While this 2 Gyr difference is statistically significant in terms of the statistical uncertainties, it is not clear whether this difference is significant when considering the systematic uncertainties. Regardless, these fields all have strong initial bursts of star formation and their overall SFHs are quite similar.

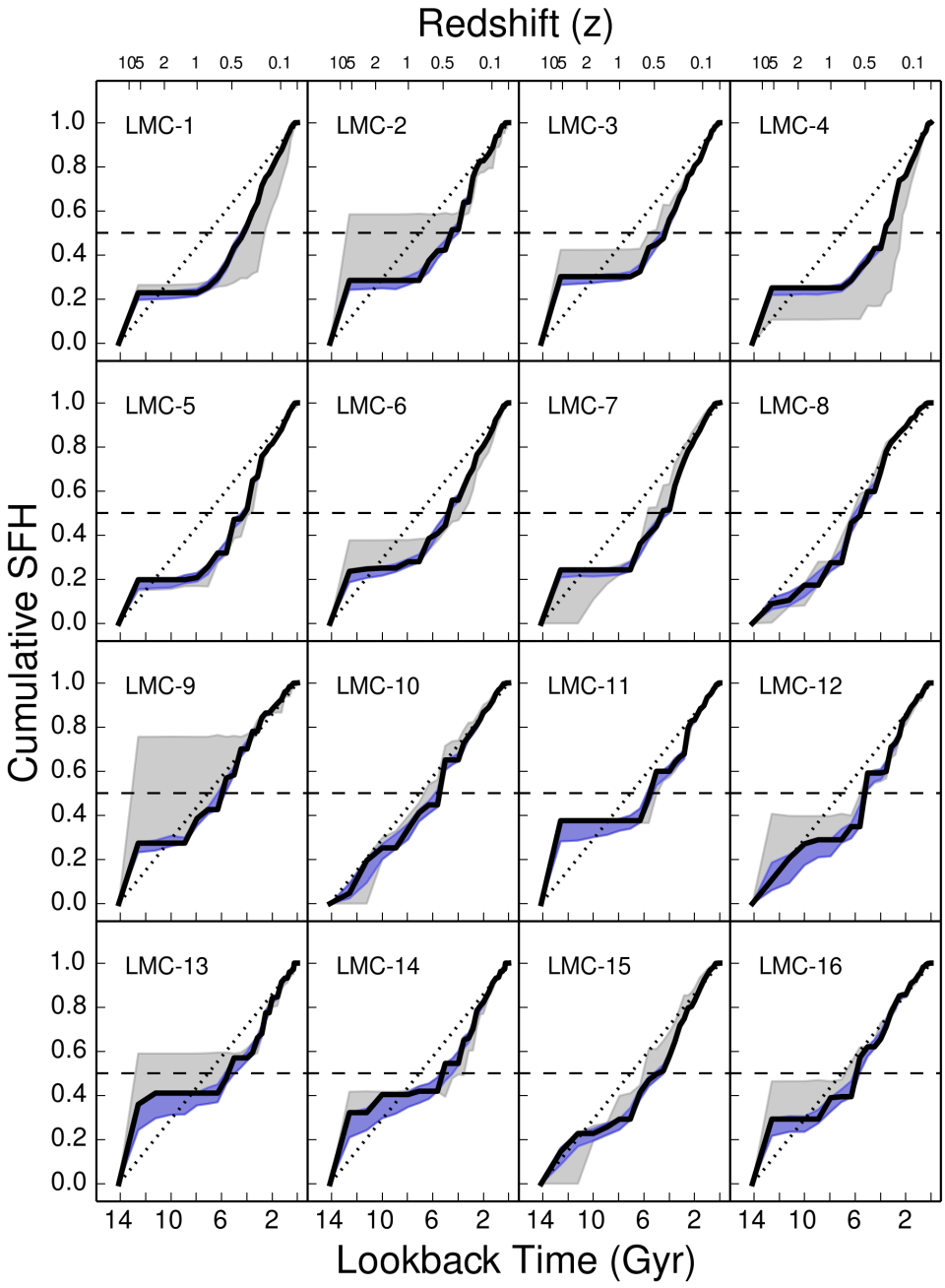

Figure 2.6: The normalized cumulative SFHs of individual fields in the LMC. The blue envelopes represent the statistical uncertainties, and the grey envelopes represent the total uncertainties, including the statistical and systematics. The dotted line represents an average constant SFR, and the dashed line shows the point at which half of the total stellar mass was formed.

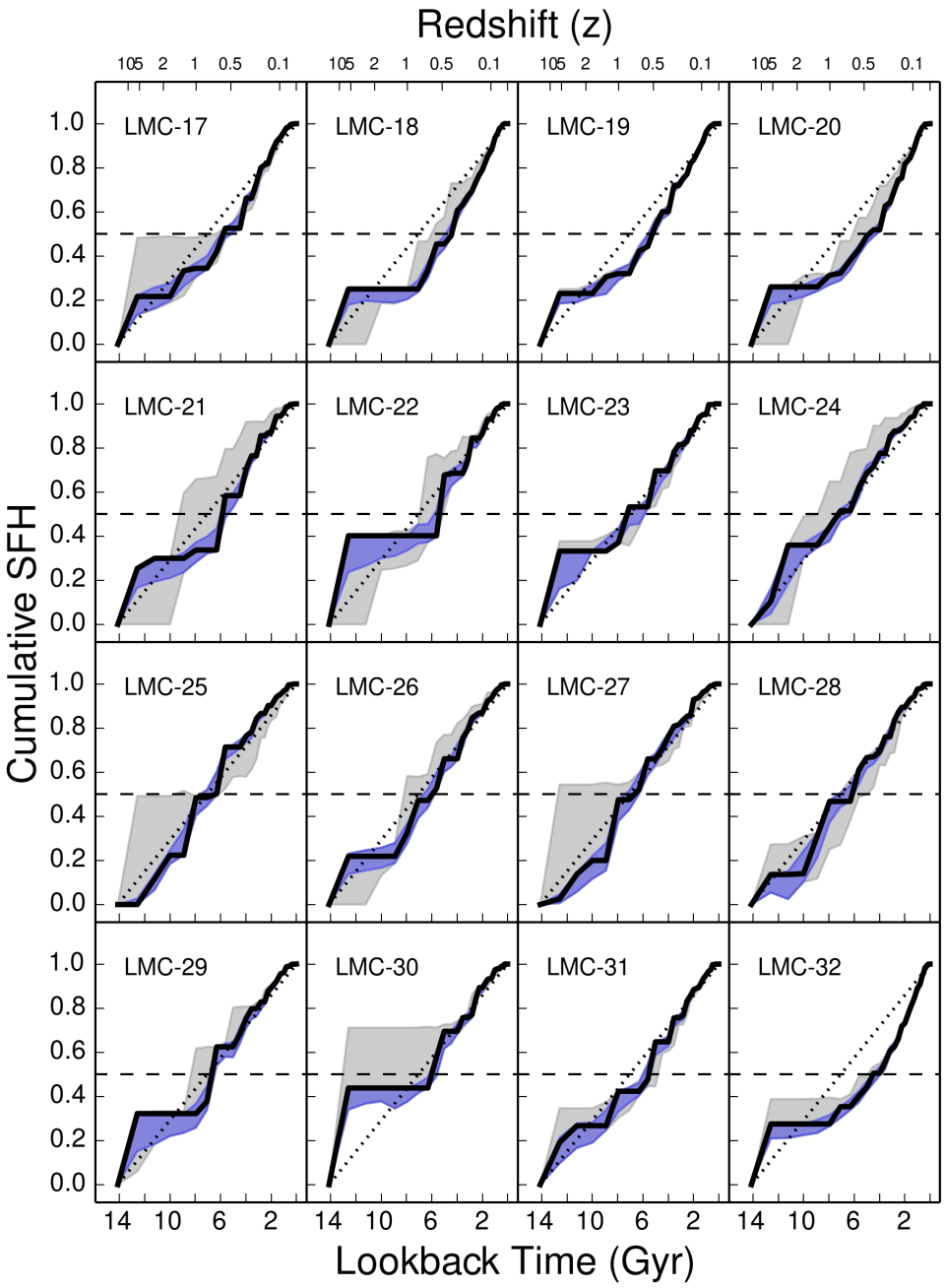

Figure 2.6: cont'd

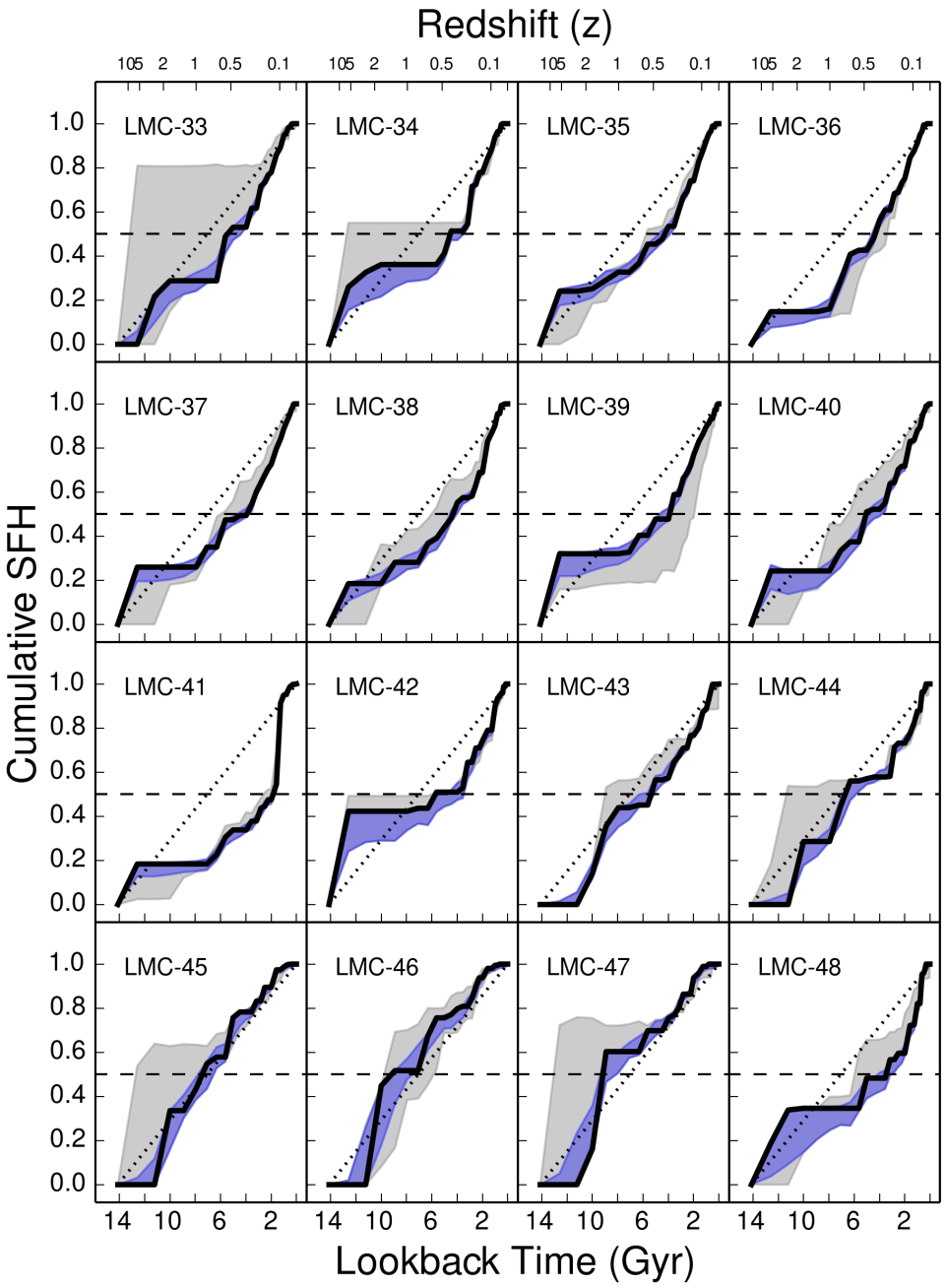

Figure 2.6: cont'd

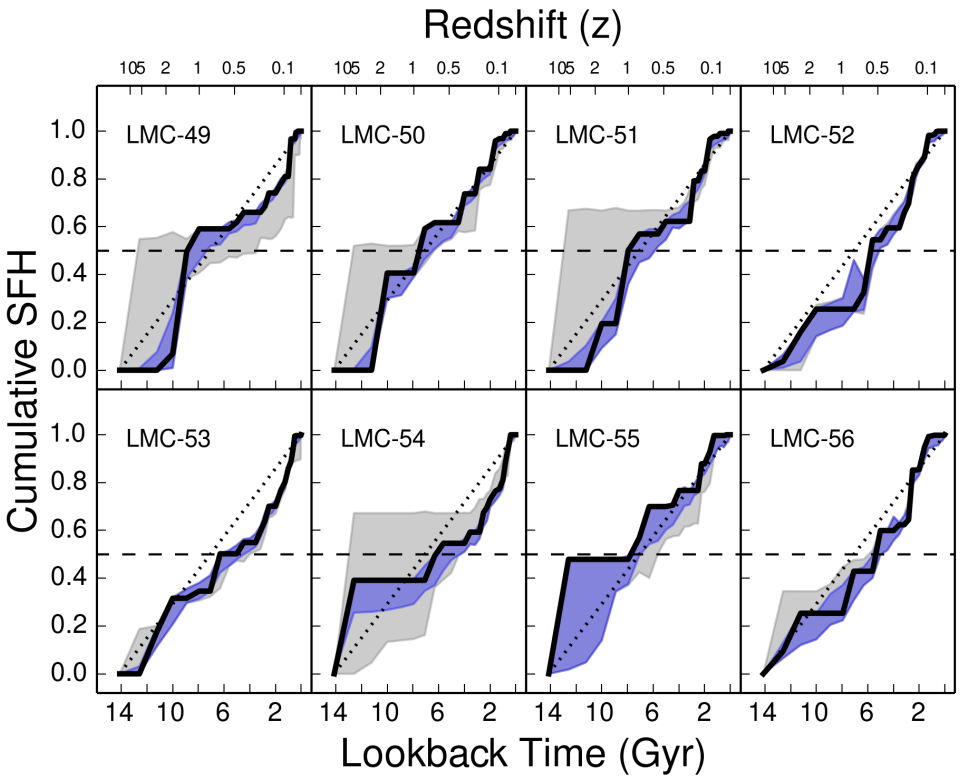

Figure 2.6: cont'd

The second group of fields also began forming stars $\sim$ 14 Gyr ago, but simply formed stars at a relatively constant rate throughout their entire histories. LMC-10 is an excellent example of this population, which also includes fields like LMC-27, LMC-28, and LMC-31. All of these fields experience some increases and decreases of their SFRs at various times, but overall, their SFRs are much closer to constant than other fields in the galaxy.

A third group of fields are those in the outer regions of the galaxy that did not experience the same early burst of star formation $\sim$ 14 Gyr ago, forming virtually no stars until 2 Gyr later, 10–12 Gyr ago. This population, including fields LMC-43, LMC-44, LMC-47, LMC-48, and others also experienced a large burst of star formation at this later time. This first burst of star formation was more significant in these outer fields, as well, forming 40% to 60% of their total stellar mass. After this period of relatively rapid star formation, their SFRs slowed. From 2 Gyr ago to present, the SFR of these fields has greatly diminished, and there is presently little to no active star formation. Other fields, notably fields LMC-21–29, also exhibit a decrease in SFR at recent times, but it is most pronounced in the outer parts of the galaxy.

While many of the sample fields can be placed in one of these three categories relatively easily, a few are more ambiguous. These categories are also somewhat spatially segregated: the first is most common among inner regions, the second is most common among fields at medium galactocentric radii, and the last is virtually exclusive to the outer parts of the galaxy. Again, however, there is some mixing. It is also interesting that fields of the first type can be found throughout the galaxy, including in the very outer regions, like LMC-54, but the third category is absent until at least 3 kpc from the galactic center.

Importantly, the biggest difference between these three categories is the amplitude of the initial burst. The significance of the initial burst is greatest in the inner parts of hte galaxy and becomes less significant with increasing galactocentric radius; thus, it is likely that the initial burst occurred in the center of the galaxy. Approximately 6 Gyr ago, a second event occurred that dramatically increased the SFR throughout the galaxy.

The SFR in the outer regions has slowed significantly in the last 2 Gyr. That is not surprising because we expect the gas and other material necessary to form stars to be

much denser in the central region of the galaxy. While star forming material is depleted in the outer region, slowing the SFR, there is still enough material in the center of the galaxy for star formation to continue.

2.4.3 Star formation histories of individual SMC fields

The SFHs of the SMC fields in our sample, shown in Figure 2.7, tend to be significantly different from the LMC fields. It is clear that the SMC did not experience a significant initial burst of star formation ~ 14 Gyr ago like the LMC. In fact, the inner regions of the SMC seem to have experienced very little star formation at all before ~ 6 Gyr ago. Before that time, all the fields except SMC 4–7 formed less that one quarter of their total stellar mass, and most fields had formed 10% or less.

Similar to the LMC, the SFR throughout the galaxy dramatically increased about 6 Gyr ago. From ~ 6 Gyr ago to the present, the SFR has remained relatively constant in virtually all the fields in our sample.

The interesting outlier of our study is SMC-4–7. Like the rest of the SMC fields, there was no significant burst of star formation beginning 14 Gyr ago, but while the SFR in the rest of the SMC increased about 6 Gyr ago, SMC-4–7 experienced a similar enhancement almost 4 Gyr earlier, around 10 Gyr ago. From 10–4 Gyr ago, the SFR in SMC 4–7 was quite constant, but then it dramatically slowed around 4 Gyr ago. SMC-4–7 experienced a history qualitatively similar to the other fields in the SMC, but this field experienced all the major features about 4 Gyr earlier than the rest of the galaxy.

SMC-4–7 is ~ 2.2–2.4 kpc from the center of the SMC, about 2 times farther than any other fields in the sample. The obvious decrease in SFR in this field, beginning around 2 Gyr ago, suggests that the outer regions of the SMC are running out of star forming material. It is likely that gas from the outer regions of the SMC has been funnelled into more central regions, allowing star formation to continue in regions nearer to the center of the SMC. We have no other fields at similar radii, so it is possible that this is just a local phenomenon, but it is reasonable to postulate that gas has been removed from the outer part of the SMC, decreasing the SFR.

While only the LMC experienced a large burst of star formation around 14 Gyr ago, both the LMC and SMC experienced some event around 6 Gyr ago that dramatically

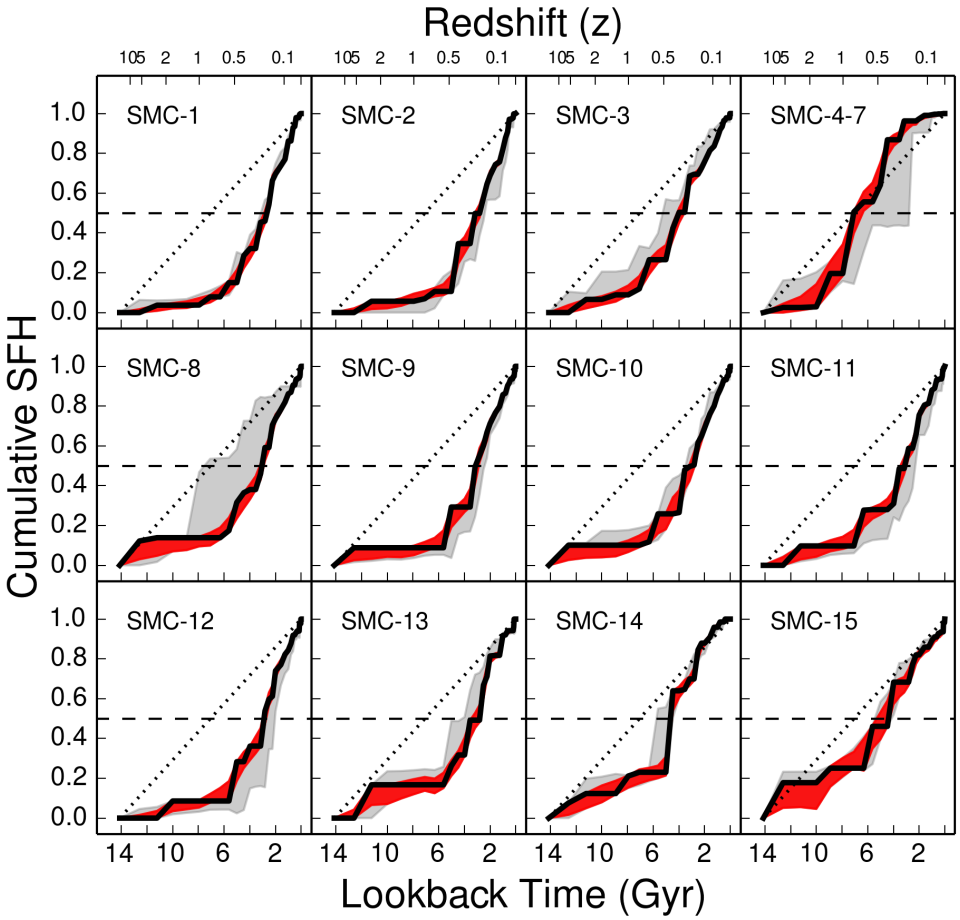

Figure 2.7: The normalized cumulative SFHs of individual fields in the SMC. The red envelopes represent the statistical uncertainties, and the grey envelopes represent the total uncertainties, including the statistical and systematics. The dotted line represents an average constant SFR, and the dashed line shows the point at which half of the total stellar mass was formed.

increased the SFR in both galaxies. In the most recent 2 Gyr, both galaxies have also been experiencing a decrease in the SFR in their outer regions, though the more centrally located regions continue to make stars.

2.5 Global SFHs

A major goal of this work is to combine the SFHs of many individual *HST* / WFPC2 fields into an approximate global SFH for each the SMC and the LMC. As a first pass, we adopt the simplest method: summing the stellar mass formed in each time bin across all the individual fields. In spite of its simplicity, this method is a good starting point because it yields the correct global solution in the case where the galaxy is uniformly sampled in its entirety. While that is not the case in our study, our spatially diverse fields do cover a representative sample of central, disk, and halo regions in each galaxy. This method of simple summing is also justified by the first order similarities of the derived SFHs in each galaxy. Because the SFHs for the different fields are so similar, applying different weighting schemes to derive a global SFH only results in subtle differences.

2.5.1 Comparing the global SFHs of the LMC and SMC

Figure 2.8 shows the global SFHs of the LMC and SMC, respectively, determined by a simple summation. As mentioned in Section 2.4.2, the LMC experienced a much more significant initial burst of star formation 14–12 Gyr ago, yielding about one quarter of the galaxy's total stellar mass, before settling into a period of relative quiescence. In the same time frame, the SMC formed only a few percent of its total stellar mass.

From 12 Gyr ago to 6–8 Gyr ago, both galaxies hosted very little star formation. The LMC only formed an additional $\sim 10\%$ of its mass, and the SMC formed even less of its total stellar mass. At 6–8 Gyr ago, both galaxies experienced an increase in the rate of star formation that continued until recent times. In about half of its lifetime, the LMC formed $\sim 70\%$ of its total stellar mass, and the SMC formed $\sim 90\%$ of its total stellar mass. Except for the initial burst of star formation present in the LMC and absent in the SMC, the two galaxies have experienced quite similar SFHs.

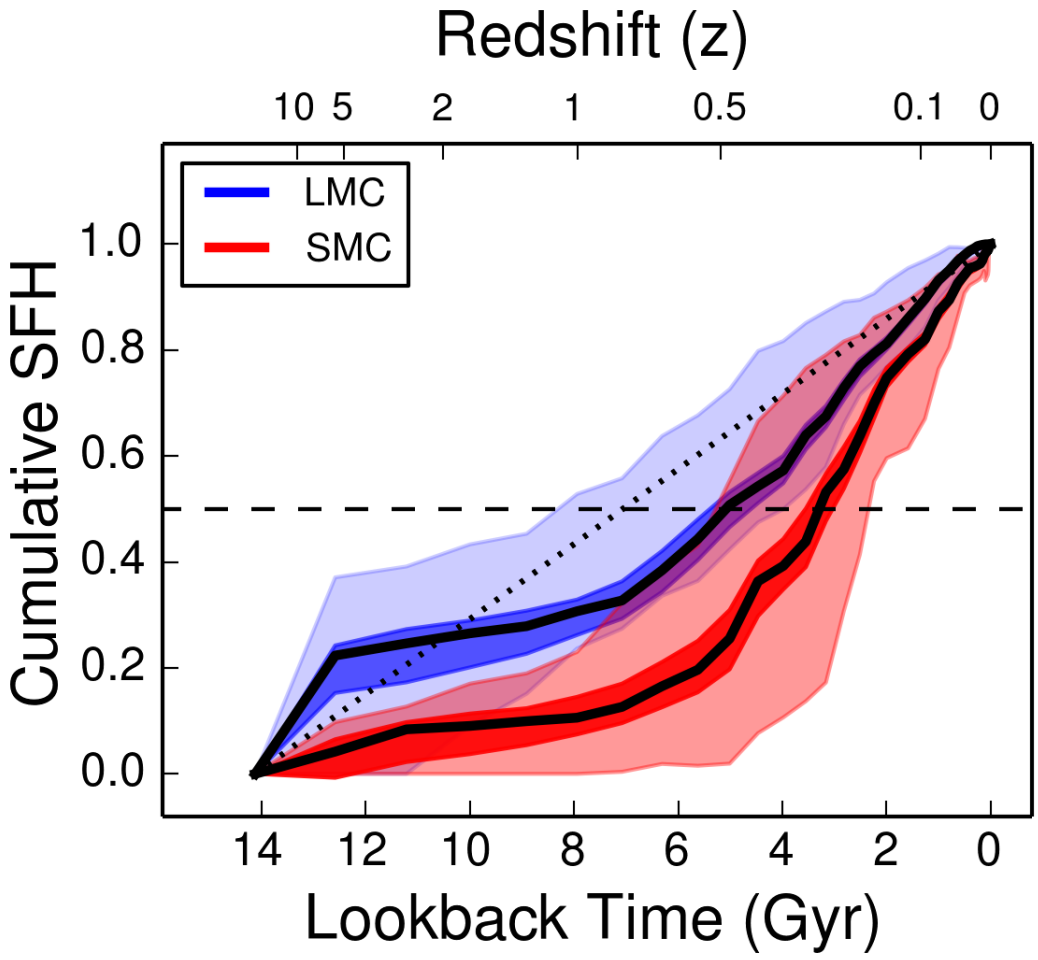

Figure 2.8: The normalized approximate global SFHs of the LMC and SMC. These SFHs were calculated by summing the stellar mass created in all fields in each individual time bin. The darker blue and red envelopes represent the statistical uncertainties of the LMC and SMC, respectively. The lighter blue and red envelops represent the total uncertainties, including statistical and systematic.

2.5.2 Comparison to previous studies

Comparison to the MCPS Results

The most widely utilized SFHs of the MCs (Harris & Zaritsky, 2004, 2009, hereafter HZ04 and HZ09) come from comprehensive spatial, but unavoidably shallow, ground-based photometry from the Magellanic Cloud Photometric Survey (MCPS; Zaritsky et al., 2002, 2004). Significant crowding effects severely compromise the depth of the MCPS CMDs, such that the oldest detected main sequence stars are $\sim$ 5 Gyr old, despite the close proximity of the MCs. Consequently, the SFHs of the MCs older than 5 Gyr are based solely on number densities of red giant branch stars, a reliance that introduces significant systematic biases into the measured SFHs (Weisz et al., 2011).

In Figure 2.9, we compare our results for the SMC with the results presented in HZ04. In their calculation of the ancient SFH of the SMC, HZ04 find that the galaxy formed $\sim$10% of its mass by $\sim$10 Gyr ago and $\sim$30% of its total stellar mass by 8 Gyr ago. In contrast, our results show that the SMC formed only $\sim$10% of its total stellar mass by 8 Gyr ago, one third the amount reported by HZ04. Our data show that it took the SMC another 3 Gyr, until $\sim$5 Gyr ago, to form 30% of its total stellar mass.

After that initial burst, HZ04 found relatively little star formation activity from 3 to 8.4 Gyr ago, which is in stark contrast to our findings. We also find a period of relatively little star formation, but our findings show that period beginning 10–12 Gyr ago and ending 6–8 Gyr ago, much earlier than HZ04's findings.

Aside from the significant discrepancy in SFR at the earliest times, our results track relatively well with HZ04's. After 8 Gyr ago, the HZ04 SFR slows significantly, and more closely matches our findings for the SFR at that time. By 3–4 Gyr ago, the two SFHs overlap nearly perfectly.

The outstanding depth of our photometry and relative lack of depth in HZ04 make our solutions significantly more robust for the oldest time bins. Therefore, it is much more likely that there was not a significant early burst of star formation in the SMC. However, the small number of fields observed in the SMC compared to the complete coverage of the MCPS, raises the question whether these differences are due to the difference in coverage. Inspection of Figure 2.7 makes this highly unlikely. Most of the SFHs in Figure 2.7 are quite similar, and *none* of the *HST* fields in the SMC produce

SFHs which are similar to that derived by HZ04. There is no evidence of a delayed and dominant first burst like that derived by HZ04 in any of the fields in Figure 2.7.

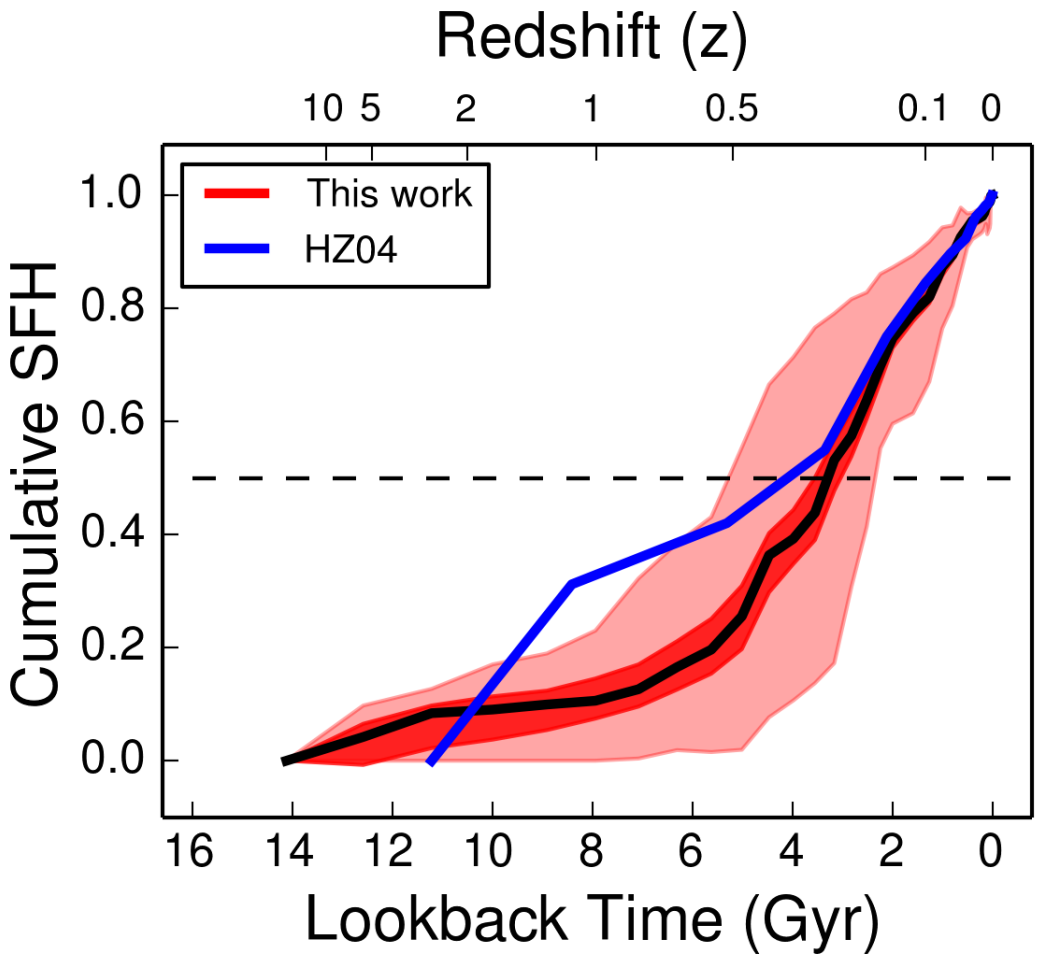

Figure 2.9: Comparison of our results for the SFH of the SMC with HZ04

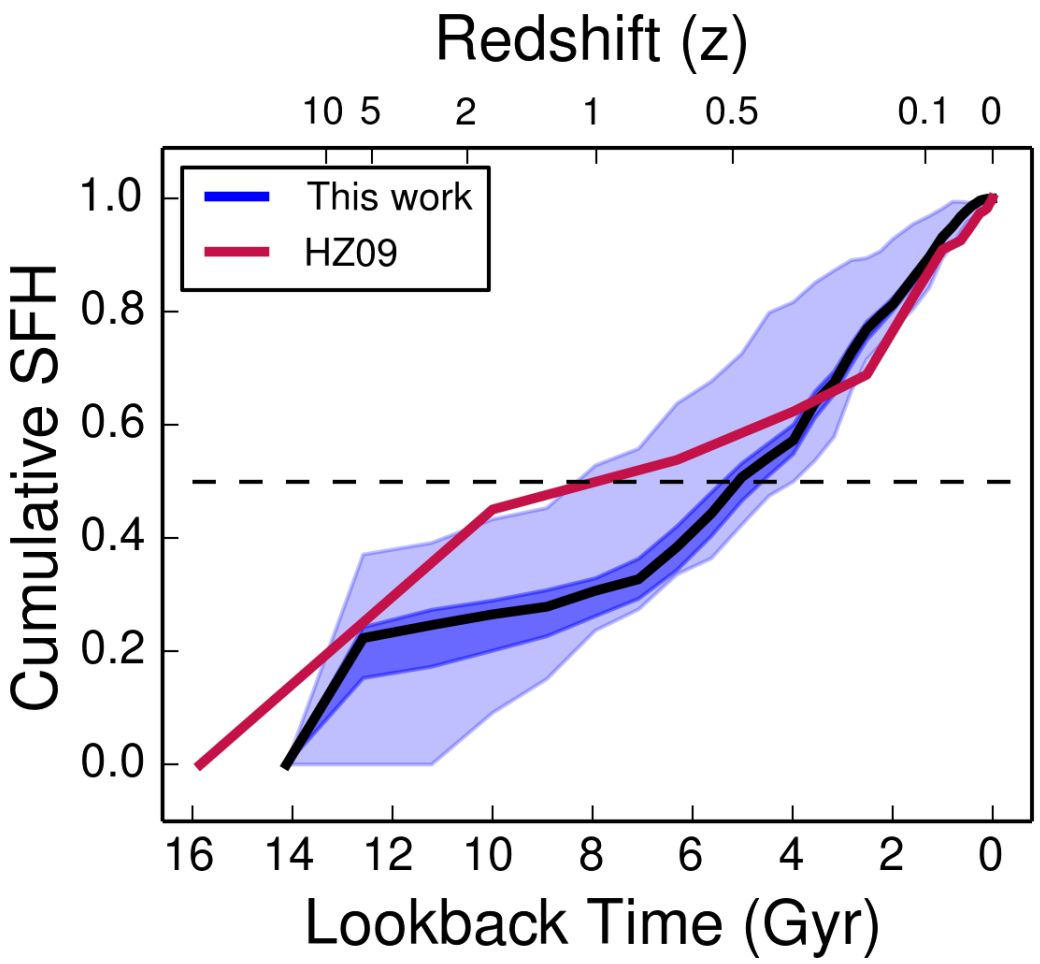

Figure 2.10: Comparison of our results for the SFH of the LMC with HZ09

In Figure 2.10, we compare our global LMC SFH to that of HZ09. Similar to HZ04 in the SMC, HZ09 have over-predicted the total star formation that occurred before ∼8 Gyr ago. By 8 Gyr ago, HZ09 find that the LMC has formed half of its stellar mass, which is nearly double what our data show. We find that the LMC had formed 25%–30% of its total stellar mass by 8 Gyr ago, and it took the LMC until 5–6 Gyr to form half of its total mass.

This discrepancy is likely due to HZ09's poor temporal resolution in the oldest time bins. Our data show an initial burst of star formation, with an SFR similar to that found by HZ09. In fact, both studies find that 20%–25% of the mass in the LMC formed by 13 Gyr ago. However, our results show that burst ending 13 Gyr ago, at which point the SFR dropped dramatically, while HZ09's data do not have the temporal resolution to make the same determination. Rather, they show that high-SFR burst continuing for another 3 Gyr, leading them to greatly over-predict the mass formed by 10 Gyr ago.

By 10 Gyr ago, the two SFHs are qualitatively quite similar, and by 4–6 Gyr ago, they fall well within agreement with one another and continue to track each other until the present. Aside from the disagreement over the initial burst, the features in these two solutions are a satisfactory match.

Comparison to other studies

Similar to HZ09, previous *HST*-based SFH studies of the LMC have found that 50% of the total stellar mass was formed $\sim 5--6$ Gyr ago, and that the SFR rose dramatically $\sim 3--4$ Gyr ago (e.g., Geha et al., 1998; Holtzman et al., 1999; Olsen, 1999; Smecker-Hane et al., 2002). While we also find that 50% of the total stellar mass was formed $\sim 5--6$ Gyr ago, our data do not show the enhancement in SFR $\sim 3--4$ Gyr ago. It should be noted that these four studies used much smaller samples (essentially individual fields), so it is possible that the enhancement they noticed did not occur throughout the galaxy. If that is the case, we would not expect to see such an enhancement in our global SFH.

Bertelli et al. (1992) examined data from three LMC fields and used synthetic CMDs and luminosity functions to model the SFH of the galaxy. They claim that very little star formation activity took place in the galaxy until about 4 Gyr ago. At that time, a "burst" event took place, dramatically increasing the SFR in the galaxy, and the

elevated SFR persisted until the present. In contrast, we find significant star formation early in the life of the LMC, but it was short lived. After a long period of quiescence, the SFR in the LMC increased dramatically $\sim$ 6 Gyr ago. Our result is remarkably similar to that of Bertelli et al. (1992), especially considering the relatively rudimentary tools they used to conduct their study over 20 years ago.

Based on extensive simulations, Kerber et al. (2009) present a process for recovering the SFH of the LMC using data from the VISTA Survey of the Magellanic System (VMC, Cioni et al., 2008). VMC uses deep near-infrared imaging to provide photometry that reaches below the oldest MSTO over the bulk of the LMC. Rubele et al. (2012) use the methodology developed by Kerber et al. (2009) and analyze four tiles from the early observations from the early observations of the VMC survey. They observed peaks in the SFR of the LMC at $\sim$ 2 Gyr ago and $\sim$ 5 Gyr ago. They suggest that the earlier peak was likely caused by an interaction with the MW, and the later peak was caused by an interaction with the SMC, as suggested by modelling (Bekki & Chiba, 2005). Our results certainly agree with their findings of a peak in SFR at $\sim$ 5 Gyr ago, but the later peak is not obviously present in our data. It will be interesting to compare to their results when the LMC is fully observed.

Cignoni et al. (2012) have obtained *HST*/Advanced Camera for Surveys (ACS) imaging and presented analyses of two fields in the SMC bar. Their derived SFHs for the two fields are quite similar and thought to be representative of the SFH for the inner SMC. Our global SFH for the SMC looks quite similar to the SFHs derived for their fields. They find that the SFR was relatively constant until 5 Gyr ago, and only about 20% of the total stellar mass was formed at that point. At 5 Gyr ago, they find a significant increase in SFR, which again remains relatively constant until the present.

Dolphin et al. (2001) presented *HST* and ground-based photometry for a field located 2° northeast of NGC 121, in the outer regions of the SMC. They found the SFH to be broadly peaked, with the maximum SFR occurring 5–8 Gyr ago, and a notable increase in SFR $\sim$ 8 Gyr ago. We find a similar increase in the SFR, but significantly later, at $\sim$ 6 Gyr ago. The most notable discrepancy is that Dolphin et al. (2001) find that over 50% of the total stellar mass is formed by 6 Gyr ago, and our results show that it took until $\sim$ 4 Gyr ago for the SMC to form 50% of its stellar mass.

Fields SMC-4–7 in this work are the same fields as studied by Dolphin et al. (2001),

and we have calculated SFHs using a very similar method, so it is no surprise that their results are nearly identical to what we find for SMC-4–7. It is also no surprise that the outer regions of the galaxy should be more dominated by an older population of stars.

McCumber et al. (2005) also utilized *HST*/WFPC2 data to analyze a population of field stars in the wing of the SMC. They find that the population was largely formed at a nearly continuous SFR from 4–12 Gyr ago with another significant burst of star formation occurring in very recent times, producing stars as young as 100 ± 10 Myr old.

Chiosi & Vallenari (2007) derived SFHs for three SMC fields near clusters at galactocentric radii varying from 0.22 kpc to 0.9 kpc. They found a very recent enhancement in the SFR, occurring < 0.5 Gyr ago, and a second enhancement 3–6 Gyr ago. They also noted that the SFR was quite low until ~ 6 Gyr ago. These findings are in excellent agreement with our own, as we find very little star formation before ~ 6 Gyr ago.

Noël et al. (2009) derive SFHs for 12 fields in the outskirts of the SMC, based on deep photometry that reaches below the oldest MSTO. They find several periods of enhancement in the SFR. The most obvious enhancement is peaked at $\sim 4 - -5$ Gyr ago, and two less significant peaks at $\sim 1.5 - -2.5$ Gyr ago and ~ 10 Gyr ago. Our SFHs also show a moderate enhancement at 4–5 Gyr ago, but the other two are not apparent in our data. It should be noted that their data come from well outside the center of the SMC. It is possible that the outskirts of the galaxy experienced a slightly different history than the central regions.

For the SMC, previous HST-based studies found that the SMC formed 50% of its stellar mass around 3–4 Gyr ago and experienced a dramatic increase in SF 3.5–4 Gyr ago (e.g., Noël et al., 2009; Cignoni et al., 2012), both similar results from Harris & Zaritsky (2004). The SFHs of the outer regions ($R > 3$ kpc) of the SMC also show a similar increase in SF 8–9 Gyr ago (e.g., Dolphin et al., 2001; Noël et al., 2009) to our SFH.

2.6 Spatially Resolved features of the LMC

2.6.1 Radial gradients in the LMC

As we have noticed in our analysis of the individual LMC fields (see Section 2.4.2), there are significant differences in the SFHs at different galactocentric radii. To gain a better

understanding of those differences, we have broken the LMC up into four annuli and combined the SFHs of all the fields in each annulus according to the method discussed in Section 2.5. The result is a combined SFH for each annulus, which more clearly illustrates the differences between the SFHs in the inner and outer parts of the LMC.

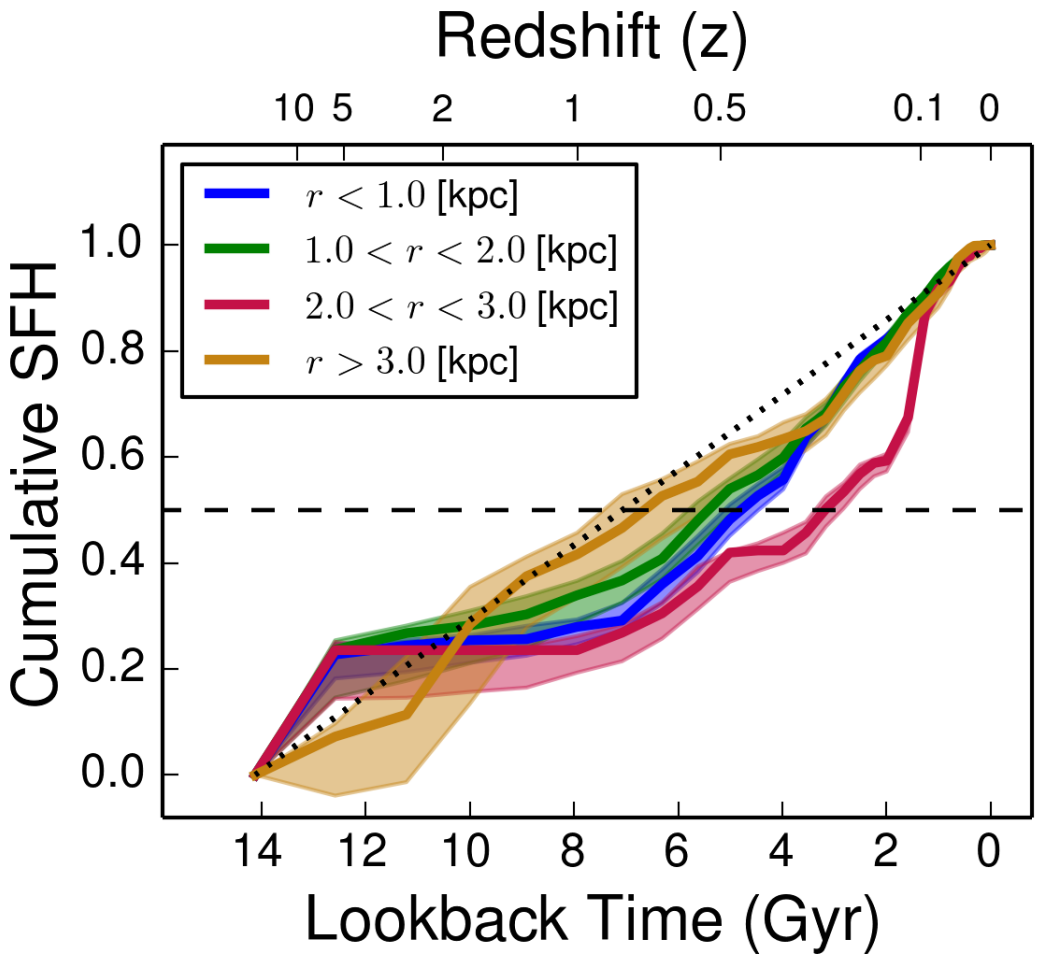

Figure 2.11: For each annulus, we have summed the stellar mass created in all fields that land within that annulus. The error envelopes represent only the statistical uncertainties. When systematic uncertainties are also included, it is clear that there is no significant discrepancy present among the annuli; i.e., there is no significant radial gradient. The dotted line represents an average constant SFH, and the dashed line illustrates when 50% of the total stellar mass was formed in each annulus.

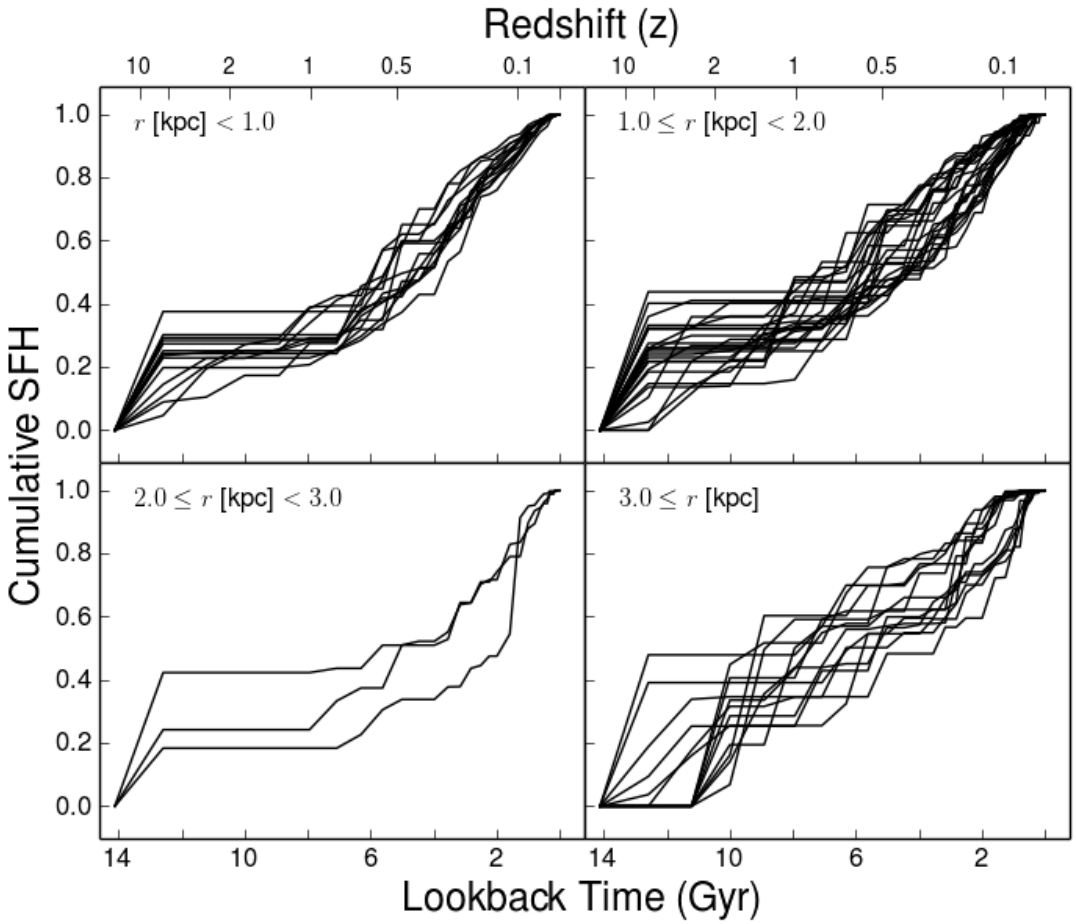

Figure 2.12: In each panel, we have plotted all of the SFHs of all of the individual fields that land in the respective annulus. For each annulus, the combination of all of SFHs yielded the result seen in Figure 2.11. It is important to note the large variations in SFH present in each panel, especially in the outermost regions of the galaxy.

In Figure 2.11, we have divided the fields into 4 annuli, each 1 kpc in width. The SFHs of the two innermost annuli ($r < 1.0$ kpc and $1.0 \leq r < 2.0$ kpc) are very similar. A little farther out, at $2.0 \leq r < 3.0$ kpc, the SFH is similar to the inner 2.0 kpc, but at ~ 5 Gyr ago, the SFR slowed at $2.0 \leq r < 3.0$ kpc compared to the inner 2.0 kpc. Between 2 and 1 Gyr ago, the SFR in the outer region increased and allowed it to catch up to the inner region. After ~ 1 Gyr ago, all the annuli within 3 kpc experienced a very similar SFH.

Beyond 3 kpc, the SFH looks quite different than it does in the rest of the LMC. The initial burst of star formation that formed $\sim 20\%$ of the total stellar mass inside of 3 kpc had a much less significant effect in the outer parts of the LMC. However, around 10–12 Gyr ago, star formation became much more vigorous in the outer parts of the galaxy. That later increase of the SFR allowed the outer part of the LMC to form a much more significant percentage of its total stellar mass than the inner 3 kpc formed in the same time-frame. By 2–4 Gyr ago, all of the regions in the LMC experienced very similar SFHs.

At first, we found the lack of an initial burst odd because it implies that there are fewer old stars in the outer parts of LMC. To look more closely, we plotted all of the SFHs of the individual fields in each annulus on the same set of axes, which is shown in Figure 2.12. While there is some dispersion among the SFHs in each annulus, the dispersion in the most ancient time bins is widest in the outermost region, which implies two important things.

First, while Figure 2.11 makes it appear as though there are virtually no old stars in the outer region, that is not the case. Looking at the SFHs of the individual constituent fields, it is clear that, in fact, some fields have formed as much as 30%–50% of their total stellar mass before 12 Gyr ago. The combined SFH was likely dominated by fields that formed a large number of stars in more recent times, driving down the fractional contribution of the older stars.

Second, the large discrepancy in the oldest time bins could mean that the stellar populations in the outer regions are not that well mixed. In some parts of the galaxy, the outer region is dominated by intermediate-age and young stars, but in other parts, the age distribution is quite different.

Third, because of the strong radial gradient in the surface brightness of the LMC, the

total number of stars formed per field is a strong function of radius. This means that recent star formation, which can be quite stochastic, has a proportionally stronger impact on the normalized SFH for the outer fields. This may be reflected in the larger variety in the SFHs of the outer fields shown in Figure 2.12. Alternatively, this may simply be due to the smaller numbers of stars in the CMDs resulting in larger uncertainties.

There are several studies that focus on the outer reaches of the LMC (e.g., Saha et al., 2010; Cioni et al., 2008), and it would be an interesting exercise to use data from such studies, with good coverage of the LMC halo, to search for discrepancies in the age distribution of the stellar populations in various parts of the halo. It is possible that we could find that the outer regions are not well mixed, which would lead to such discrepancies. In either case, more thorough coverage would allow us to minimize any ambiguity.

It would be useful to re-examine these findings with a larger data set containing more fields in the outer portion of the LMC. While we have tried to avoid contamination by selecting fields that contain only the fields population of stars, it is possible that some bias exists in our sample, artificially increasing the number of younger stars in these outer fields.

2.6.2 The LMC Bar

We thought it would be interesting to examine the effects the LMC bar has on the global SFH of the LMC, especially in the innermost 1 kpc. Figure 2.13 shows the SFH of the innermost 1 kpc as well as the SFHs of just the fields that are in the bar, and the fields that are not in the bar.

To determine which fields lie in the LMC bar, we overlaid Spitzer $4.5\mu m$ contours (Meixner et al., 2006) on our map of the LMC (see Figure 2.1). First, we smoothed the flux using a 200 pixel ($\sim$ 4 arcmin) kernel. We then defined the bar to have $F_{4.5\mu m} > 0.3$ MJy/str. The fields that land inside that boundary are LMC 1–7 and LMC 11–14. Fields LMC-13 and LMC-14 are slightly beyond the 1 kpc cut-off, so they were excluded.

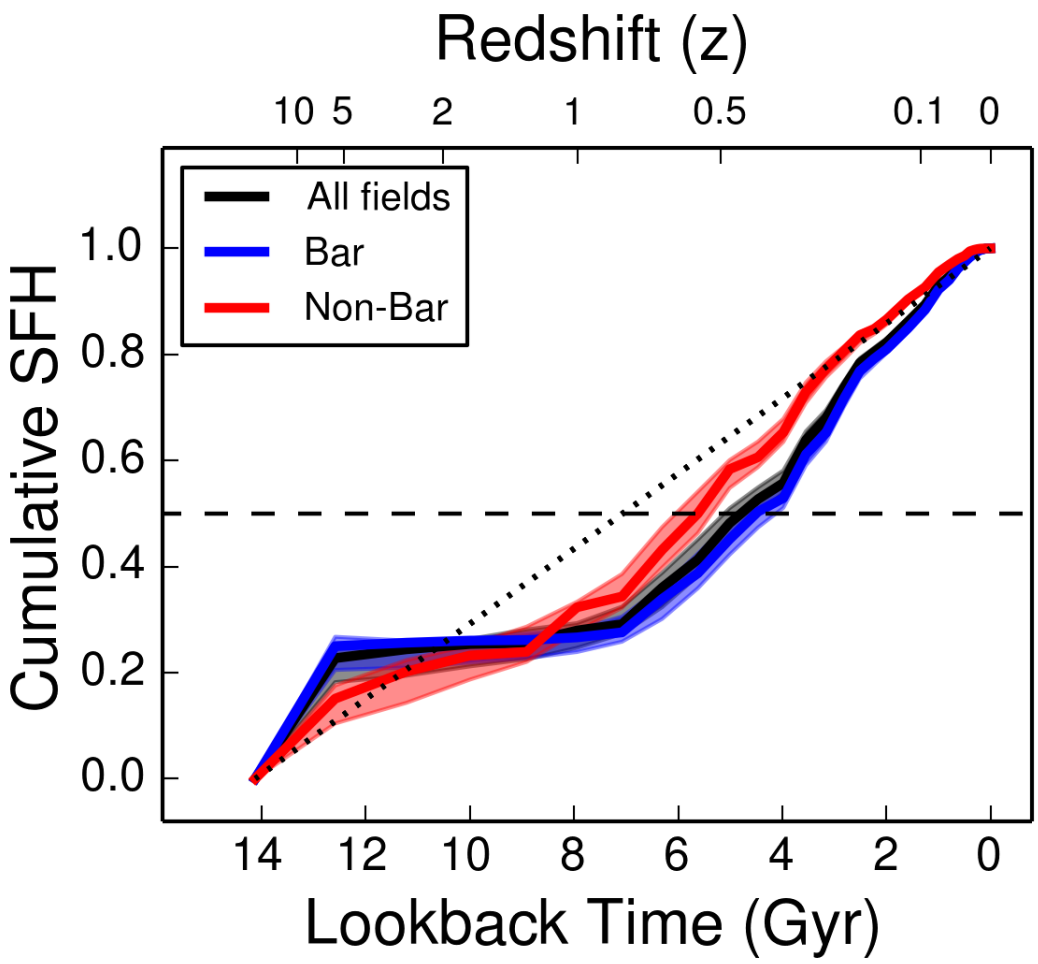

Figure 2.13: Using all of the fields where $r < 1.0$ kpc, we have broken them up into bar and non-bar components. Bar fields were selected to be fields that fell inside the region where 4.5 μm flux is greater than 0.3 MJy/str (Meixner et al., 2010). The error envelopes represent only statistical uncertainties. The addition of systematic uncertainties shows that there is no significant discrepancy present among the populations shown here. Within the innermost kpc, the bar is the dominant feature. We see this effect because the SFH of all fields with $r < 1.0$ kpc very closely tracks the SFH of the bar fields. However, there is not a significant difference between the SFHs of the bar and non-bar fields.

The bar fields and all of the fields in the inner 1 kpc have nearly identical SFHs, indicating that the bar is quite a dominant feature in this range. It is possible that some bias exists because only five fields in the innermost 1 kpc lie outside the bar, compared to nine field in the bar. However, the bar is definitely a dominant component in this part of the galaxy, so it is not a surprise to see that the SFH of the inner 1 kpc matches that of the bar.

The non-bar fields formed slightly less of the fractional stellar mass in early times compared to the bar counterparts. They did not experience the initial burst quite as strongly as the fields in the bar. At about 8 Gyr ago, the non-bar fields experienced an increase in SFR that the bar fields did not. After that event, the non-bar fields had formed more of their fractional mass than the bar, which continued until the recent past. Within the last 1 Gyr, the SFR in the non-bar fields has decreased slightly relative to the bar. Overall, the non-bar fields experienced a more constant SFR than the bar, but the SFH of the bar fields more closely matches the SFH of the entire galaxy.

2.7 The Magellanic Clouds' cluster population

While we have specifically avoided clusters when choosing the sample for this study, it is important to consider the cluster populations of the Magellanic Clouds when considering their global SFHs. Clusters contain a significant amount of mass, and their contribution to the total mass of their host galaxy is likely non-negligible. However, because so much mass is contained in such a small area, including them in our sample would greatly bias the results. The SFH of the whole galaxy would appear to trace that of the cluster population. By examining the literature, we can consider known ages of the cluster populations of the LMC and SMC without contaminating our sample. There is a large on-going debate in astronomy concerning whether the star formation rates for field stars are the same as the stellar cluster formation rates.

There is a well known age gap in the cluster population of the LMC; few clusters seem to have formed in the LMC between about 3 and 9 Gyr ago (Geisler et al., 1997). As more and more LMC clusters are thoroughly studied, some clusters are being found to lie in that gap (e.g., Sarajedini, 1998).

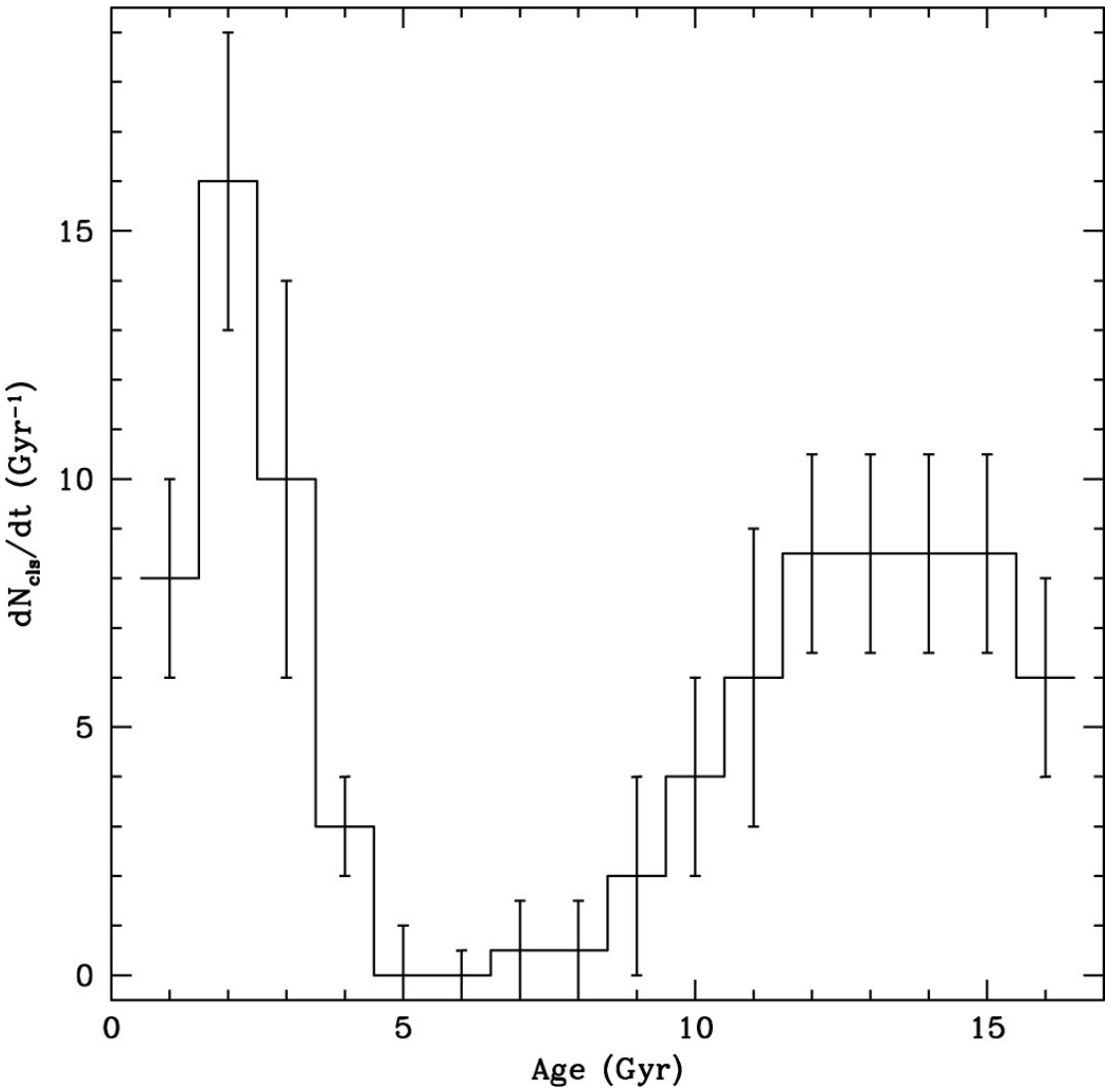

Figure 2.14: Figure 10 from Piatti et al. (2011): The intrinsic age distribution of 45 well-known LMC clusters older than 1 Gyr

Piatti et al. (2011) conducted analysis on 45 LMC clusters, comparing the age distribution of the clusters to the SFH of the LMC. They found satisfactory agreement with Harris & Zaritsky (2009), except for an excess of clusters at the oldest times. We have reproduced their cluster age distribution in Figure 2.14. This distribution shows active cluster formation from ancient times until about 10 Gyr ago before reaching the age gap, where very little cluster formation occurred. Then, around 4 Gyr ago, the cluster formation rate increased again, and peaked 2 Gyr ago.

Our SFH of the LMC shows some similar behaviour. The SFR is relatively high at very early times before dropping around 12 Gyr ago. After a period of relatively little star formation, the SFR increased again around 6 Gyr ago. The timing between the SFR and cluster formation rate does not quite line up, but they exhibit similar features. In fact, the star formation in the LMC seems to have experienced a history very similar to the clusters, but the field population experienced these feature about 2 Gyr before the clusters.

Interestingly, the SMC lacks clusters as old as the oldest clusters in the LMC and the MW. The oldest known cluster in the LMC, NGC 121, is estimated to be only 10.5 Gyr old (Glatt et al., 2008), compared to the 12–12.5 Gyr old of the oldest clusters in the LMC and MW (Dotter et al., 2010). This result is interesting because it is similar to our findings in the field population. We notice a significant burst of star formation activity in the LMC 12–14 Gyr ago that appears absent in the SMC. The SMC does not seem to contain many older stars at all.

In a study of the 15 SMC clusters, in addition to 35 others from literature, Parisi et al. (2014) found a peak in the cluster formation rate at around 5 Gyr ago. In this study, we found that the SFR in the SMC increased significantly 4–6 Gyr ago, which is in excellent agreement with their result. The elevated rate of cluster formation continues to present time, which also matches our result that after the SFR increased 4–6 Gyr ago, it maintained the elevated rate until the present.

2.8 Implications for evolutionary scenarios for the Magellanic Clouds

The origins of the Magellanic clouds remain somewhat mysterious, but detailed ancient SFHs can help discriminate between plausible and implausible theories. Our deep photometry has allowed us to derive SFHs with excellent temporal resolution, even at the most ancient times. We can, therefore, begin to discern likely evolutionary scenarios of the MCs.

The first obvious feature in Figure 2.8 is the discrepancy in the SFHs of the LMC and SMC at the earliest times. The LMC experienced a significant burst of star formation, but the SMC did not. Therefore, it is likely that the MCs did not originally form together, but began interacting some time in the more recent past. The difference between the early evolution of the SMC and LMC could simply be a reflection of the differences in their masses. Galaxies with masses comparable to the LMC or greater all appear to have dominant early episodes of star formation. Less dominant early star formation or delayed star formation is observed in lower mass galaxies. This would imply that the early evolution of the LMC and SMC was determined more by their masses than by interactions.

Star formation events can be triggered or enhanced by tidal encounters with other galaxies, so a well-constrained SFH can be a useful tool to determine the likelihood of such interaction in the past. By matching patterns of star formation to interaction timings predicted by dynamical models, we can discern the plausibility of those models. In the case of the MCs, we are interested in two possible situations: the MCs interacting with each other, and the MCs interacting with the MW.

Because star formation is enhanced by tidal interactions, it seems unlikely that either of the MCs experienced a significant encounter before 6–8 Gyr ago. The SFR in both galaxies is quite low over this period of time, and there is no evidence of the type of burst that would likely be caused by an interaction.

At 6–8 Gyr ago, there is a sudden, significant increase in the SFR in both the LMC and the SMC. It is plausible that a tidal interaction triggered new star formation at this time, and it is interesting that a similar burst occurred a about the same time in both galaxies. If the MCs did not originally form together, it is plausible that their first

encounter with each other occurred at that time, greatly enhancing the SFR in both galaxies. It is also possible that this is when the pair first encountered the MW.

Our data do not reveal any periodic behavior in the SFH of either the LMC or SMC. We would expect each passage through the Milky Way to induce an elevated SFR in one or both of the MCs, and if the Clouds have orbited several times, one would expect to see periodic elevations in the SFR in our SFHs. While we cannot definitively claim that the MCs have not been orbiting the MW for a long time, it is likely that they are on their first passage (e.g., Besla et al., 2007; Boylan-Kolchin et al., 2011; Busha et al., 2011). This is in agreement with the recent kinematic reconstructions of their orbits (Kallivayalil et al., 2006a,b, 2013; Besla et al., 2007, 2010).

2.9 Summary

We have presented results from an *HST* archival program focused on constraining the ancient SFHs of the field population of the MC. Photometry and AST data for 56 LMC fields and 15 SMC fields observed with *HST*/WFPC2 were obtained from LOGPHOT and used to calculate SFHs for all of the fields in the study. Many previous studies of the MCs have typically utilized ground-based data to achieve comprehensive spatial coverage or space-based data to reach the photometric depth needed to calculate accurate SFHs back to the most ancient times. Our archival approach has yielded photometry significantly deeper than the oldest MSTO, allowing for accurate measurements of the ancient SFH, as well as excellent spatial coverage of a diverse and representative sample of fields.

Previous studies have often only considered the LMC or the SMC, making it exceedingly difficult to directly compare the SFHs of the two galaxies. Our self-consistent methods, applied to both galaxies, allow us to easily compare the histories of the LMC and SMC to each other.

By summing the SFHs of the individual fields, we calculated an approximate global SFH of each galaxy. Our accurate view of the ancient star formation activity has shown that there was a significant burst of star formation at a very early time (12–14 Gyr ago) in the LMC that was absent in the SMC, making it unlikely that the two galaxies formed together. After 12 Gyr ago, the SFHs of the two galaxies were very similar.

They both experienced very little star formation until 6–8 Gyr ago, at which time the SFR increased significantly in both galaxies. It is possible that this even was triggered by tidal interaction with each other and/or the MW.

We also considered the possibility of radial gradients in the LMC, but our findings were inconclusive. There is evidence that the initial burst of star formation in the LMC was constrained to the inner regions, but a definitive trend is not obvious. We were also unable to find evidence of radial gradients in the SMC, but our small sample size prevents us from making definitive claims.

We found no periodic behavior in the SFH of either the LMC or SMC. Therefore, we conclude that the MCs are likely on their first pass through the MW. It is highly unlikely that they have been in bound orbits for a significant portion of their lifetimes because successive tidal encounters would be evident in their fossil records.

We note qualitative similarities between the SFHs derived here and the cluster formation histories (Piatti et al., 2011; Glatt et al., 2008; Parisi et al., 2014). In both populations, the LMC experienced early formation activity, followed by a long period of quiescence, before resuming formation activity again, which continues to the present. These features occur 2 Gyr earlier in the SFH than they do in the cluster formation history. In both the cluster formation history and the SFH of the SMC, there was relatively little activity until about 5 Gyr ago, at which time formation activity in both field and cluster populations increased dramatically.

Upon comparison of our results to Harris & Zaritsky (2004) and Harris & Zaritsky (2009) we find agreement in recent times, but discrepancies in the ancient SFHs. The Harris & Zaritsky (2004) and Harris & Zaritsky (2009) photometry is much shallower than the photometry presented here, so we propose that ancient SFHs presented here should be favored.

Acknowledgements

Support for this work was provided by NASA through grant number HST GO-12853 from the Space Telescope Science Institute, which is operated by AURA, Inc., under NASA contract NAS5-26555. This research made extensive use of NASAs Astrophysics Data System Bibliographic Services.

Table 2.1. The observational properties of the LMC and SMC fields

Field number (1)	Field name (2)	RA (J2000) (3)	DEC (J2000) (4)	*HST*-ID (5)	Galactocentric radius (kpc) (6)	70% completeness M_{F555W} (7)	M_{F606W} (8)	M_{F814W} (9)	Distance Modulus (10)	Foreground A_V (mag) (11)	Differential A_V (mag) (12)	M_{total} $10^5 M_\odot$ (13)
LMC-1	u4b115	5:22:55	-69:44:51	GO-7382	0.05	+6.60	···	+5.60	18.35	0.20	0.05	3.25
LMC-2	u4b112	5:22:57	-69:46:53	GO-7382	0.05	+6.70	···	+5.70	18.35	0.10	0.30	3.49
LMC-3	u2o901	5:24:17	-69:46:50	GO-6229	0.06	+6.30	···	+5.50	18.30	0.15	0.20	3.64
LMC-4	u4b113	5:23:57	-69:49:26	GO-7382	0.06	+6.60	···	+5.70	18.35	0.20	0.10	3.02
LMC-5	u4b114	5:24:03	-69:51:16	GO-7382	0.09	+6.60	···	+5.60	18.35	0.20	0.00	3.29
LMC-6	u4zn05	5:25:03	-69:47:56	GO-7306	0.11	+6.30	···	+5.20	18.35	0.20	0.10	3.56
LMC-7	u4zn06	5:20:15	-69:14:58	GO-7306	0.50	+6.50	···	+5.40	18.40	0.20	0.05	2.83
LMC-8	u4zn03	5:26:19	-70:21:02	GO-7306	0.55	+6.70	···	+5.50	18.40	0.15	0.00	2.23
LMC-9	u4zn02	5:16:37	-70:28:52	GO-7306	0.80	+7.00	···	+5.80	18.40	0.15	0.10	1.23
LMC-10	u65006	5:24:06	-68:48:48	GO-8676	0.81	+7.00	···	+6.00	18.40	0.25	0.10	1.38
LMC-11	u6mi30	5:35:33	-69:21:21	GO-9428	0.96	+5.90	···	+4.80	18.45	0.25	0.30	1.45
LMC-12	u2hw04	5:35:22	-69:16:18	GO-5753	0.97	+6.40	···	+5.40	18.50	0.30	0.30	1.34
LMC-13	u6e806	5:36:01	-69:17:30	GO-9111	1.01	+6.20	···	+5.30	18.45	0.30	0.40	1.24
LMC-14	u6m706	5:36:01	-69:17:28	GO-9343	1.01	+6.20	···	+5.30	18.45	0.30	0.45	1.29
LMC-15	u3y501	5:34:40	-70:24:42	GO-5901	0.98	+7.20	···	+6.10	18.40	0.20	0.05	1.83
LMC-16	u4zn01	5:17:19	-70:46:44	GO-7306	0.98	+6.90	···	+5.80	18.45	0.10	0.15	0.99
LMC-17	u4zn08	5:33:57	-70:51:11	GO-7306	1.20	+6.90	···	+5.70	18.40	0.15	0.10	1.17
LMC-18	u65008	5:06:38	-69:20:26	GO-8676	1.31	+7.20	···	+6.10	18.40	0.25	0.15	1.26
LMC-19	u65002	5:05:49	-69:43:25	GO-8676	1.31	+7.00	···	+6.00	18.40	0.25	0.10	1.52
LMC-20	u4zn04	5:03:58	-69:33:04	GO-7306	1.47	+6.80	···	+5.70	18.40	0.25	0.00	1.39
LMC-21	u4b110	5:11:40	-71:09:50	GO-7382	1.47	+7.00	···	+6.10	18.45	0.05	0.40	0.65
LMC-22	u4b109	5:11:57	-71:11:16	GO-7382	1.48	+6.90	···	+6.00	18.45	0.00	0.55	0.61
LMC-23	u4b108	5:12:13	-71:12:38	GO-7382	1.48	+6.90	···	+6.00	18.45	0.00	0.50	0.68
LMC-24	u4b107	5:13:02	-71:16:44	GO-7382	1.50	+7.00	···	+6.00	18.40	0.15	0.00	0.60

Table 2.1 (cont'd)

Field number (1)	Field name (2)	RA (J2000) (3)	DEC (J2000) (4)	*HST*-ID (5)	Galactocentric radius (kpc) (6)	70% completeness M_{F555W} (7)	M_{F606W} (8)	M_{F814W} (9)	Distance Modulus (10)	Foreground A_V (mag) (11)	Differential A_V (mag) (12)	M_{total} $10^5 M_\odot$ (13)
LMC-25	u4b103	5:10:10	-71:10:12	GO-7382	1.54	+6.90	···	+5.90	18.45	0.10	0.00	0.59
LMC-26	u4b102	5:10:26	-71:11:34	GO-7382	1.55	+6.90	···	+6.00	18.45	0.10	0.10	0.58
LMC-27	u4b101	5:10:42	-71:12:57	GO-7382	1.55	+6.90	···	+6.00	18.45	0.15	0.00	0.59
LMC-28	u4b104	5:10:58	-71:14:19	GO-7382	1.55	+6.90	···	+6.00	18.45	0.10	0.15	0.57
LMC-29	u4b105	5:11:14	-71:15:41	GO-7382	1.56	+7.00	···	+6.10	18.45	0.10	0.20	0.63
LMC-30	u4b106	5:11:31	-71:17:03	GO-7382	1.56	+7.00	···	+6.00	18.45	0.10	0.30	0.62
LMC-31	u65005	5:06:20	-70:58:21	GO-8676	1.62	+7.00	···	+6.10	18.45	0.15	0.20	0.62
LMC-32	u4zn07	5:01:11	-69:07:16	GO-7306	1.77	+6.80	···	+5.70	18.40	0.20	0.05	1.25
LMC-33	u63s03	5:02:19	-68:34:13	GO-8576	1.91	+7.00	···	+6.10	18.45	0.10	0.40	1.02
LMC-34	u63s01	5:01:56	-68:37:20	GO-8576	1.91	+7.00	···	+6.00	18.40	0.05	0.55	1.02
LMC-35	u63s04	5:01:44	-68:38:53	GO-8576	1.91	+7.00	···	+6.10	18.40	0.20	0.15	1.01
LMC-36	u63s05	5:01:32	-68:40:26	GO-8576	1.91	+7.00	···	+6.10	18.40	0.15	0.20	1.02
LMC-37	u63s06	5:01:20	-68:41:59	GO-8576	1.91	+7.00	···	+6.10	18.40	0.25	0.05	1.07
LMC-38	u65003	5:45:23	-71:08:45	GO-8676	1.96	+7.10	···	+6.00	18.35	0.20	0.30	0.92
LMC-39	u65004	4:57:18	-69:27:26	GO-8676	1.97	+7.00	···	+5.90	18.40	0.30	0.30	0.87
LMC-40	u65007	4:54:23	-70:01:58	GO-8676	2.16	+7.00	···	+6.00	18.45	0.30	0.00	0.60
LMC-41	u65001	5:02:18	-68:00:26	GO-8676	2.22	+7.10	···	+6.00	18.40	0.15	0.10	0.92
LMC-42	u2o902	5:58:18	-68:20:51	GO-6229	2.91	+7.80	···	+7.00	18.35	0.20	0.05	0.23
LMC-43	u4ax38	5:03:02	-66:24:06	GO-7307	3.30	+7.70	···	+6.60	18.35	0.05	0.10	0.34
LMC-44	u4ax29	5:03:24	-66:20:33	GO-7307	3.33	+7.30	···	+5.80	18.35	0.05	0.05	0.33
LMC-45	u4ax73	5:28:51	-73:30:27	GO-7307	3.23	+7.30	···	+5.80	18.45	0.20	0.00	0.22
LMC-46	u4ax82	5:27:19	-73:32:51	GO-7307	3.25	+7.70	···	+6.80	18.40	0.10	0.25	0.23
LMC-47	u4ax75	5:29:47	-73:38:01	GO-7307	3.34	+8.50	···	+7.10	18.45	0.10	0.20	0.18
LMC-48	u4ax01	5:01:28	-66:01:33	GO-7307	3.65	+7.10	···	+5.80	18.45	0.15	0.25	0.26

Table 2.1 (cont'd)

Field number (1)	Field name (2)	RA (J2000) (3)	DEC (J2000) (4)	*HST*-ID (5)	Galactocentric radius (kpc) (6)	70% completeness M_{F555W} (7)	M_{F606W} (8)	M_{F814W} (9)	Distance Modulus (10)	Foreground A_V (mag) (11)	Differential A_V (mag) (12)	M_{total} $10^5 M_\odot$ (13)
LMC-49	u4ax10	5:01:41	-66:00:10	GO-7307	3.66	+7.70	···	+6.70	18.30	0.00	0.10	0.22
LMC-50	u4ax93	6:12:53	-69:49:00	GO-7307	3.63	+7.70	···	+6.70	18.40	0.10	0.00	0.14
LMC-51	u4ax86	6:15:07	-69:48:55	GO-7307	3.80	+8.50	···	+7.30	18.30	0.05	0.15	0.13
LMC-52	u4ax84	6:15:44	-69:48:23	GO-7307	3.84	+7.20	···	+5.80	18.50	0.10	0.05	0.14
LMC-53	u4ax20	5:10:19	-65:26:48	GO-7307	3.84	+7.80	···	+6.80	18.35	0.10	0.05	0.25
LMC-54	u2c501	5:14:44	-65:17:42	GO-5208	3.88	+8.00	···	+6.90	18.35	0.05	0.25	0.22
LMC-55	u4ax27	5:55:52	-73:55:01	GO-7307	4.15	+7.80	···	+6.80	18.30	0.20	0.25	0.13
LMC-56	u4ax22	5:57:37	-73:57:33	GO-7307	4.24	+8.50	···	+7.20	18.40	0.15	0.00	0.12
SMC-1	u2o903	0:55:37	-73:04:20	GO-6229	0.34	+7.55	···	+6.55	18.85	0.25	0.15	1.33
SMC-2	u46c01	0:46:40	-72:44:43	GO-6860	0.48	+7.65	···	+6.55	18.80	0.20	0.20	1.15
SMC-3	u65c06	0:45:41	-72:52:20	GO-8654	0.55	+5.65	···	+5.35	18.80	0.20	0.15	1.23
SMC-4	u37704	0:45:54	-70:34:43	GO-6604	2.43	···	···	···	···	···	···	···
SMC-5	u377a4	0:46:06	-70:46:44	GO-6604	2.22	···	···	···	···	···	···	···
SMC-6	u377a6	0:48:54	-70:32:44	GO-6604	2.42	···	···	···	···	···	···	···
SMC-7	u37706	0:48:54	-70:47:43	GO-6604	2.16	···	···	···	···	···	···	···
SMC-4-7	u377	···	···	···	···	+7.05	···	+6.15	18.95	0.20	0.00	0.30
SMC-8	u4woge	0:55:11	-72:30:13	GO-8059	0.39	···	+6.35	+5.65	18.85	0.20	0.30	1.13
SMC-9	u4wogd	0:55:27	-72:30:38	GO-8059	0.40	···	+6.25	+5.55	18.85	0.20	0.30	1.10
SMC-10	u4wog3	0:57:59	-72:35:07	GO-8059	0.48	···	+6.25	+5.55	18.80	0.25	0.40	1.06
SMC-11	u4wodp	1:01:43	-72:43:33	GO-8059	0.71	···	+6.95	+6.05	18.80	0.20	0.20	0.80
SMC-12	u4woeo	0:57:54	-72:11:39	GO-8059	0.78	···	+7.05	+6.25	18.85	0.15	0.35	0.78
SMC-13	u4woav	1:02:59	-72:34:55	GO-8059	0.84	···	+6.55	+5.85	18.95	0.15	0.45	0.66
SMC-14	u27z67	0:40:22	-72:43:58	GO-5091	0.97	···	+6.95	+5.75	18.80	0.25	0.00	0.79
SMC-15	u4wodx	1:14:05	-73:24:20	GO-8059	1.74	···	+6.65	+5.85	18.85	0.30	0.20	0.20

Table 2.1 (cont'd)

Field number (1)	Field name (2)	RA (J2000) (3)	DEC (J2000) (4)	*HST*-ID (5)	Galactocentric radius (kpc) (6)	70% completeness M_{F555W} (7)	M_{F606W} (8)	M_{F814W} (9)	Distance Modulus (10)	Foreground A_V (mag) (11)	Differential A_V (mag) (12)	M_{total} $10^5 M_\odot$ (13)

Note. — The fields have been sorted approximately by galactocentric radius, but fields in near spatial proximity to each other have been grouped together. The extinction values listed in columns 8 and 9 were derived from CMD fitting as described in Section 2.3. The total stellar mass formed in each field (i.e. the integral of the SFH) is listed in column 10. As indicated, SMC fields 4–7 were combined to form a single, larger field, SMC-4–7.

Chapter 3

Future Work

3.1 Testing Stellar Evolution Models

The ability to test the robustness of the SFHs derived in this work would provide great insight no only to the quality and reliability of the results presented here, but also to our ability to derive accurate SFHs in general. By analyzing the data presented here using three different sets of stellar models (Padua (Girardi et al., 2010), BaSTI (Pietrinferni et al., 2004), and Dartmouth (Dotter et al., 2008)), we could perform just such a test. We have already analyzed the data using the Padua models, so all that remains is to use the BaSTI and Dartmouth models and compare the results.

The choice of stellar models is known to introduce biases into SFHs recovered from shallow CMDs that do not include the ancient MSTO. However, preliminary tests indicate that for deep CMDs, including the ancient MSTO, the solutions converge (e.g., Weisz et al., 2011, 2012). Thus, we expect the models to produce consistent SFHs. However, a comparison between these three sets of widely used models has never been conducted on CMDs as deep as those presented in this thesis. Agreement among the solutions would validate the consistency of the models, while conflicting SFHs would suggest that underlying model physics may need to be revisited. The addition of a relatively small amount of analysis could, therefore, have important implications for stellar models.

3.2 A Quantitative star formation history of And II

A great deal of my time as a graduate student was spent trying to reduce and analyze ground-based photometry data of the dwarf spheroidal galaxy, Andromeda II (And II). The data were taken on the Suprimecam on the Subaru telescope (Miyazaki et al., 2002), and originally published as aperture photometry by McConnachie et al. (2007).

Upon close examination of the partially reduced data, I discovered that distortions in the images caused by the atmosphere were not properly accounted for. Much effort has been spent to find a method to reduce and analyze the data using DOLPHOT and MATCH to solve for the photometry and derive the SFH.

Studying And II and devising methods for studying other dwarfs in the Andromeda system could greatly advance our understanding of dwarf galaxies and the make up of larger galaxies. And II is a particularly complex dwarf, containing multiple stellar components and a broad RGB. Not only do these properties contradict the former paradigm of dwarf galaxies as simple systems with singular populations, And II provides a good testing ground for our methods because of its complexity.

The calculation of a quantitative SFH of a dwarf galaxy in the Andromeda system utilizing ground-based data would be an important step forward because it would allow us to continue to use a similar method to analyze data from other galaxies, including those in the Andromeda system. Ground-based instruments, and their wide fields-of-view, carry the benefit of being able to observe entire dwarf galaxies in a single pointing, though they are not capable of achieving the photometric depth of space-based instruments. I hope to be able to utilize the comprehensive spatial coverage of the Subaru data to derive a global SFH of And II. Ultimately, I hope to be able to combine the photometric depth of carefully selected *HST* observations with the coverage of the Subaru data to derive a SFH that both covers the whole galaxy and provides excellent temporal resolution, even in the oldest time bins.

3.3 The star formation histories of the Andromeda dwarf population

The Local Group is dominated by two major spiral galaxies. At first glance, there is a lot in common between the Milky Way and Andromeda galaxies. They are both spiral galaxies with well-defined spiral arms. They have similar masses with both galaxies weighing in between $1 - 2 \times 10^{12} M_{\odot}$ (Watkins et al., 2010). They also have similar luminosities with $L_V \sim 2.0 \times 10^{10} L_{\odot}$ for the Milky Way and $L_V \sim 2.6 \times 10^{10} L_{\odot}$ for Andromeda (van der Kruit, 1989).

The systems of dwarf galaxies orbiting M31 and the Milky Way are structurally somewhat different, but the distribution of these galaxies around M31 and the Milky Way are quite similar. All satellites of Andromeda with a distance less than 200 kpc are of early type, but farther out from the galaxy, there is a mixture of early and late type satellites (van den Bergh, 2006; Grebel, 1999). In general, Milky Way satellites behave similarly, and only early type objects are found close to the main disk. McConnachie & Irwin (2006) also show that dSphs with higher central surface brightnesses are systematically found closer to their hosts in both systems. Mateo (1998) suggests that this could be due to an observational bias, but McConnachie & Irwin (2006) claim the effect is real. These distributions suggest that environment plays a key role in the evolution of dwarf galaxies. The Large and Small Magellanic Clouds are glaring exceptions, but van den Bergh (2006) suggests that they could be interlopers from a much more isolated region of the Local Group.

While a distance-morphology relation seems to exist and be the same for both systems, the structures of the Andromeda satellites are somewhat different from the Milky Way dwarfs. McConnachie & Irwin (2006) examined the radial surface brightness profiles of seven Andromeda dwarfs and found that they are best fit with a King model. For Andromeda V, there is an excess of stars at large radii, which is likely explained by tidal effects (Choi et al., 2002). Irwin & Hatzidimitriou (1995) conducted similar analysis on Galactic satellites and found that six of their eight targets show a similar excess. McConnachie & Irwin (2006) suggest that this result could mean that Galactic dwarfs are more tidally disturbed because the Milky Way has a stronger tidal field than Andromeda. They also find that the scale radii of the M31 dwarfs are a factor of $2 - 3$

larger than their Galactic counterparts. (Their surface brightnesses are also lower because they are more extended.) The stronger tidal field of the Milky Way could again be the culprit, truncating the Milky Way dwarfs at smaller radii.

Both the similarities and differences in these systems suggest that environment plays a key role in dwarf galaxy morphology. Further investigation of these similarities and differences could teach us a great deal about the Local Group and galaxy formation and evolution.

A better understanding of the star formation histories (especially the early histories) of the Andromeda dwarfs could be crucial to our wider understanding of all galaxies. The relative simplicity of dwarf galaxies allows for a much more thorough study of their properties; however, to date, only the dwarf galaxies in the Milky Way system have been studied in rigorous detail. With information on only one system, we must ask whether this set is a representative sample or if it is biased. Environmental factors are likely to play a significant role in dwarf galaxy evolution, so it is likely that the Milky Way sample is not completely representative. Using observations of several of the Andromeda dwarfs (McConnachie et al., 2009) and the analysis method described above in Section 3.2, we could derive detailed, global SFHs of many of the Andromeda dwarfs. A detailed study of the Andromeda dwarfs can help us decipher how much of a role environment might play as well as what other factors affect dwarf galaxy evolution, which would have great impact theoretical models of galaxy formation and evolution.

Chapter 4

Conclusions

In this dissertation, I have spent a great deal of time discussing dwarf galaxies, their SFHs, and the ancient SFHs of two dwarf galaxies in particular: the LMC and SMC. While these two galaxies are very well studied, the work presented here represents much of the current understanding of their SFHs and improves upon the understanding of their histories at very ancient times. In this chapter, I summarize the main results of all the work presented in this thesis.

In Chapter 2, I presented a new study of the ancient SFHs of the LMC and SMC. By utilizing archival *HST*/WFPC2 data, I was able to provide good spatial coverage of both galaxies, as well as photometric depth that reached well below the oldest MSTO. These two factors, and the consistent method used to study both galaxies, allowed me to derive approximate global SFHs for each galaxy and compare them directly.

We found an initial burst of star formation in the LMC that was absent in the SMC, which could imply that the two galaxies were not formed together. There is also no evidence of periodic behavior in the SFH, implying that the Magellanic Clouds have not been orbiting the Milky Way for very long, and are likely on their first passage through the Galaxy.

A closer study of the LMC revealed no clear evidence for a radial gradient in the SFH and showed that the oldest stars might not be very well mixed through the galaxy. More analysis is necessary to constrain the mixing time scales implied by our study, but these results clearly demonstrate the power of accurate ancient SFHs in constraining evolutionary scenarios.

Chapter 3 mentioned ongoing and potential future projects related to the work in this thesis, with the overarching goal of better understanding galaxy formation and evolution.

First, I propose to expand the study of the SFHs of the Magellanic Clouds to include a comparison of three different, commonly used stellar evolution models. A comparison of these three sets of models using photometry that reaches below the MSTO has never been done, and conducting such a test could demonstrate the consistency of the models. Agreement among the solutions would validate the consistency of the models, while conflicting SFHs would suggest that underlying model physics may need to be revisited.

Next, I hope to complete work on an ongoing project to derive a quantitative SFH for And II. While I have devoted a great deal of my time as a graduate student to developing a method to properly reduce and analyze ground-based data, with the ultimate goal of producing a SFH, the process still needs to be refined and tested. Once complete, this method will yield a quantitative global SFH for And II, providing new insight into the history of a galactic system outside of the Milky Way.

Finally, I hope to expand the work on And II to other dwarf galaxies in the Andromeda system. Ground-based observations of several Andromeda dwarfs are available for analysis, and once we have developed a robust method to analyze these data, we can apply it to these other dwarf galaxies. The results of such a study would have interesting cosmological implications because it would tell us whether what we have learned from the Milky Way is applicable to other galaxies.

References

Bastian, N., & Silva-Villa, E. 2013, MNRAS, 431, L122

Bastian, N., Gieles, M., Ercolano, B., & Gutermuth, R. 2009, MNRAS, 392, 868

Bekki, K., & Chiba, M. 2005, MNRAS, 356, 680

Bertelli, G., Mateo, M., Chiosi, C., & Bressan, A. 1992, ApJ, 388, 400

Besla, G., Kallivayalil, N., Hernquist, L., et al. 2012, MNRAS, 421, 2109

Besla, G., Kallivayalil, N., Hernquist, L., et al. 2010, ApJ, 721, L97

Besla, G., Kallivayalil, N., Hernquist, L., et al. 2007, ApJ, 668, 949

Bono, G., Caputo, F., Fiorentino, G., Marconi, M., & Musella, I. 2008, ApJ, 684, 102

Bothun, G. D., & Thompson, I. B. 1988, AJ, 96, 877

Boylan-Kolchin, M., Besla, G., & Hernquist, L. 2011, MNRAS, 414, 1560

Busha, M. T., Marshall, P. J., Wechsler, R. H., Klypin, A., & Primack, J. 2011, ApJ, 743, 40

Chiosi, E., & Vallenari, A. 2007, A&A, 466, 165

Cignoni, M., Cole, A. A., Tosi, M., et al. 2012, ApJ, 754, 130

Cioni, M.-R. L., Bekki, K., Clementini, G., et al. 2008, PASA, 25, 121

Choi, P. I., Guhathakurta, P., & Johnston, K. V. 2002, AJ, 124, 310

Connors, T. W., Kawata, D., & Gibson, B. K. 2006, MNRAS, 371, 108

Dolphin, A. E. 2013, ApJ, 775, 76

Dolphin, A. E. 2012, ApJ, 751, 60

Dolphin, A. E. 2002, MNRAS, 332, 91

Dolphin, A. E., Walker, A. R., Hodge, P. W., et al. 2001, ApJ, 562, 303

Dotter, A., Sarajedini, A., Anderson, J., et al. 2010, ApJ, 708, 698

Dotter, A., Chaboyer, B., Jevremović, D., et al. 2008, ApJS, 178, 89

Gardiner, L. T., & Noguchi, M. 1996, MNRAS, 278, 191

Geha, M. C., Holtzman, J. A., Mould, J. R., et al. 1998, AJ, 115, 1045

Geisler, D., Bica, E., Dottori, H., et al. 1997, AJ, 114, 1920

Gieles, M., Bastian, N., & Ercolano, B. 2008, MNRAS, 391, L93

Girardi, L., Williams, B. F., Gilbert, K. M., et al. 2010, ApJ, 724, 1030

Glatt, K., Grebel, E. K., & Koch, A. 2010, A&A, 517, A50

Glatt, K., Gallagher, J. S., III, Grebel, E. K., et al. 2008, AJ, 135, 1106

Gordon, K. D., Meixner, M., Meade, M. R., et al. 2011, AJ, 142, 102

Grebel, E. K. 1999, The Stellar Content of Local Group Galaxies, 192, 17

Harris, J., & Zaritsky, D. 2009, AJ, 138, 1243

Harris, J., & Zaritsky, D. 2004, AJ, 127, 1531

Haschke, R., Grebel, E. K., Duffau, S., & Jin, S. 2012, AJ, 143, 48

Holtzman, J. A., Afonso, C., & Dolphin, A. 2006, ApJS, 166, 534

Holtzman, J. A., Gallagher, J. S., III, Cole, A. A., et al. 1999, AJ, 118, 2262

Irwin, M., & Hatzidimitriou, D. 1995, MNRAS, 277, 1354

James, P. A., & Ivory, C. F. 2011, MNRAS, 411, 495

Jarosik, N., Bennett, C. L., Dunkley, J., et al. 2011, ApJS, 192, 14

Kallivayalil, N., van der Marel, R. P., Besla, G., Anderson, J., & Alcock, C. 2013, ApJ, 764, 161

Kallivayalil, N., van der Marel, R. P., Alcock, C., et al. 2006, ApJ, 638, 772

Kallivayalil, N., van der Marel, R. P., & Alcock, C. 2006, ApJ, 652, 1213

Kennicutt, R. C., Jr., Bresolin, F., Bomans, D. J., Bothun, G. D., & Thompson, I. B. 1995, AJ, 109, 594

Kerber, L. O., Girardi, L., Rubele, S., & Cioni, M.-R. 2009, A&A, 499, 697

Kim, S., Staveley-Smith, L., Dopita, M. A., et al. 1998, ApJ, 503, 674

Kroupa, P. 2001, MNRAS, 322, 231

Marigo, P., Girardi, L., Bressan, A., et al. 2008, A&A, 482, 883

Marzke, R. O., & da Costa, L. N. 1997, AJ, 113, 185

Mateo, M. L. 1998, ARA&A, 36, 435

Mayer, L., Mastropietro, C., Wadsley, J., Stadel, J., & Moore, B. 2006, MNRAS, 369, 1021

McConnachie, A. W., Irwin, M. J., Ibata, R. A., et al. 2009, Nat, 461, 66

McConnachie, A. W., Arimoto, N., & Irwin, M. 2007, MNRAS, 379, 379

McConnachie, A. W., & Irwin, M. J. 2006, MNRAS, 365, 1263

McCumber, M. P., Garnett, D. R., & Dufour, R. J. 2005, AJ, 130, 1083

Meixner, M., Galliano, F., Hony, S., et al. 2010, A&A, 518, L71

Meixner, M., Gordon, K. D., Indebetouw, R., et al. 2006, AJ, 132, 2268

Miyazaki, S., Komiyama, Y., Sekiguchi, M., et al. 2002, PASJ, 54, 833

Murai, T., & Fujimoto, M. 1980, PASJ, 32, 581

Noël, N. E. D., Aparicio, A., Gallart, C., et al. 2009, ApJ, 705, 1260

Olsen, K. A. G. 1999, AJ, 117, 2244

Parisi, M. C., Geisler, D., Carraro, G., et al. 2014, AJ, 147, 71

Parker, J. W., Hill, J. K., Cornett, R. H., et al. 1998, AJ, 116, 180

Piatti, A. E., & Geisler, D. 2013, AJ, 145, 17

Piatti, A. E., Geisler, D., & Mateluna, R. 2012, AJ, 144, 100

Piatti, A. E. 2011, MNRAS, 418, L40

Piatti, A. E., Clariá, J. J., Parisi, M. C., & Ahumada, A. V. 2011, PASP, 123, 519

Pietrinferni, A., Cassisi, S., Salaris, M., & Castelli, F. 2004, ApJ, 612, 168

Popescu, B., Hanson, M. M., & Elmegreen, B. G. 2012, ApJ, 751, 122

Read, J. I., & Gilmore, G. 2005, MNRAS, 356, 107

Rubele, S., Kerber, L., Girardi, L., et al. 2012, A&A, 537, A106

Sarajedini, A. 1998, AJ, 116, 738

Sabbi, E., Gallagher, J. S., Tosi, M., et al. 2009, ApJ, 703, 721

Saha, A., Olszewski, E. W., Brondel, B., et al. 2010, AJ, 140, 1719

Searle, L., & Zinn, R. 1978, ApJ, 225, 357

Smecker-Hane, T. A., Cole, A. A., Gallagher, J. S., III, & Stetson, P. B. 2002, ApJ, 566, 239

Stanimirović, S., Staveley-Smith, L., & Jones, P. A. 2004, ApJ, 604, 176

Tollerud, E. J., Boylan-Kolchin, M., Barton, E. J., Bullock, J. S., & Trinh, C. Q. 2011, ApJ, 738, 102

Tolstoy, E., Hill, V., & Tosi, M. 2009, ARA&A, 47, 371

Udalski, A., Soszynski, I., Szymanski, M. K., et al. 2008, **??**jnlActa Astron., 58, 89

Udalski, A., Soszyński, I., Szymański, M. K., et al. 2008, **??**jnlActa Astron., 58, 329

van den Bergh, S. 2006, AJ, 132, 1571

van der Kruit, P. C. 1989, in The Milky Way as a Galaxy, Edls. G. Gilmore, I. R. King and P. C. van der Kruit

Wagner-Kaiser, R., & Sarajedini, A. 2013, MNRAS, 431, 1565

Weisz, D. R., Dolphin, A. E., Skillman, E. D., et al. 2013, MNRAS, 431, 364

Weisz, D. R., Zucker, D. B., Dolphin, A. E., et al. 2012, ApJ, 748, 88

Weisz, D. R., Dalcanton, J. J., Williams, B. F., et al. 2011, ApJ, 739, 5

Watkins, L. L., Evans, N. W., & An, J. H. 2010, MNRAS, 406, 264

Yoshizawa, A. M., & Noguchi, M. 2003, MNRAS, 339, 1135

Zaritsky, D., Harris, J., Thompson, I. B., & Grebel, E. K. 2004, AJ, 128, 1606

Zaritsky, D., Harris, J., Thompson, I. B., Grebel, E. K., & Massey, P. 2002, AJ, 123, 855

Zaritsky, D., Harris, J., & Thompson, I. 1997, AJ, 114, 1002